Pedro David Anastácio de Bastos

Licenciatura em Ciências da Engenharia Química e Bioquímica

Separation of Azeotropic Mixtures using High Ionicity Ionic Liquids

Dissertação para obtenção do Grau de Mestre em
Engenharia Química e Bioquímica

Orientador: Doutora Isabel Maria Delgado Jana Marrucho Ferreira, Investigadora Coordenadora, Laboratório de Termodinâmica Molecular, ITQB-UNL

Co-orientador: Doutora Ana Belén Pereiro Estévez, Investigadora de Pós-Doutoramento, Laboratório de Termodinâmica Molecular, ITQB-UNL

Presidente: Professor Doutora Ana Isabel Nobre Martins Aguiar de Oliveira Ricardo
Arguente: Doutor Luís Alexandre Almeida Fernandes Cobra Branco
Vogais: Doutora Isabel Maria Delgado Jana Marrucho
Doutora Ana Belén Pereiro Estévez

FACULDADE DE CIÊNCIAS E TECNOLOGIA
UNIVERSIDADE NOVA DE LISBOA

Março 2014

UNIVERSIDADE NOVA DE LISBOA

Faculdade de Ciências e Tecnologia

Departamento de Química

Separation of Azeotropic Mixtures using High Ionicity Ionic Liquids

Pedro David Anastácio de Bastos

Dissertação apresentada na Faculdade de Ciências e Tecnologia da Universidade Nova de Lisboa para obtenção do grau Mestre em Engenharia Química e Bioquímica

Orientador: Doutora Isabel Maria Delgado Jana Marrucho Ferreira
Co-orientador: Doutora Ana Belén Pereiro Estévez

2014

Separation of Azeotropic Mixtures using High Ionicity Ionic Liquids

COPYRIGHT

Pedro David Anastácio de Bastos

Faculdade de Ciências e Tecnologia

Universidade Nova de Lisboa

Agradecimentos

Após este longo e desafiante caminho, gostaria de expressar a minha sincera gratidão a quem, de todas as maneiras, me fez chegar até aqui. Um enorme agradecimento à minha orientadora Drª Isabel Marrucho por me ter dado esta oportunidade de conhecer um novo mundo profissional e por me ter acompanhado ao longo do trabalho, nunca deixando que eu sentisse que o meu trabalho não tinha valor o suficiente. Quero agradecer à minha co-orientadora Drª Ana Belén Pereiro, fundamental em ter dado o empurrão necessário para o prosseguimento do meu trabalho, nunca hesitando em disponibilizar os recursos para o alcançar.

Agradeço às pessoas do Laboratório de Termodinâmica Molecular que estiveram sempre disponíveis para me ajudar, quer a nível moral, quer a nível do próprio trabalho, nomeadamente ao Filipe Oliveira, David Patinha e Liliana Tomé.

Dedico também esta tese a várias pessoas:

Aos meus pais e avós, que lutaram incansavelmente para que eu chegasse até aqui, acreditando sempre em mim.

À Ana Santos, pessoa cujos passos admiráveis de sucesso segui durante 5 anos de faculdade, desde do dia 1 e que me ajudou a crescer e desenvolver todas as capacidades, especialmente a nível de sentido crítico.

O especial agradecimento à Catarina Florindo deve-se ao apoio incondicional de todas as formas imagináveis, desde as palavras meigas e compreensivas até à sua presença e contribuição indispensável no trabalho.

Acknowledgments

After this long and challenging road, I would like to express my sincere appreciation to those who, in every way, helped me get to this phase. I enormously thank my supervisor, Drª. Isabel Marrucho for having given me this opportunity to be a part of a new professional world and for having supervised me throughout the work, never letting me feel that it was of not enough value. I want to thank my co-supervisor Drª. Ana Belén Pereiro, fundamental in giving the necessary encouragement for the continuation of my work, never hesitating to provide the resources to achieve it.

I want to thank the people of the Laboratory of Molecular Thermodynamics that had always been available to help me, morally or in the work itself, such as Filipe Oliveira, David Patinha and Liliana Tomé.

I also dedicate this thesis to several people:

To my parents and grandparents, who fought tirelessly so that I could reach this phase, always believing in me.

To Ana Santos, whose admirable and successful footsteps I followed for 5 years in university, since day one, and who helped me grow and develop all skills, especially in analysing critically.

A special appreciation goes to Catarina Florindo, who unconditionally helped me in every way imaginable, from her sweet and understanding words to her presence and indispensable contribution to the work.

"I went to the woods because I wanted to live deliberately, I wanted to live deep and suck out all the marrow of life,
To put to rout all that was not life and not when I had come to die, discover that I had not lived"

Henry David Thoreau

Resumo

A separação de misturas azeotrópicas, para que os seus componentes possam ser reutilizados em ciclos de produção, é de particular interesse na indústria química moderna sustentável. O processo mais comum na separação de azeótropos é a destilação extractiva/azeotrópica. No entanto, dado que uma elevada pressão e altas temperaturas são requeridas é necessária uma enorme quantidade de energia para se atingir um sistema de uma fase fluída.

Na última década, os líquidos iónicos têm vindo a demonstrar a capacidade de agirem como solventes de extracção e têm vindo a crescer como uma alternativa "verde" aos solventes orgânicos na separação de azeótropos. Recentemente, os líquidos iónicos de alto carácter iónico foram desenvolvidos através da adição de um sal inorgânico a um líquido iónico e consequentemente, foi demonstrado que a ionicidade é particularmente relevante na separação eficiente de misturas azeotrópicas.

Neste trabalho, a ionicidade de três sistemas foi estudada e comparada com os líquidos puros, um dos quais constituído por um líquido iónico + sal inorgânico ($[C_2MIM][SCN]+[NH_4][SCN]$) e os restantes dois sistemas constituídos por uma mistura de dois líquidos iónicos: 1-etil-3-metilimidazólio tiocianato $[C_2MIM][SCN]$ + 1-etil-3-metilimidazólio etilsulfato $[C_2MIM][C_2SO_4]$; $[C_2MIM][SCN]$ + 1-etil-3-metilimidazólio dicianamida $[C_2MIM][DCA]$. O equilíbrio líquido-líquido para os dois sistemas ternários: etanol + heptano + ($[C_2MIM][SCN]$, ou $[C_2MIM][SCN]+[C_2MIM][C_2SO_4]$) foi determinado a 298.15 K. A selectividade e o coeficiente de distribuição foram utilizados na avaliação da viabilidade como solvente e uma correlação destes parâmetros com a ionicidade foi estabelecida

Palavras-chave Mistura Azeotrópica, Equilíbrio Líquido-Líquido, Ionicidade, Alto Carácter Iónico, Líquido Iónico, Eficiência de extracção

Abstract

The separation of azeotropic mixtures, so that their components can be reused in production cycles, is of particular interest in modern sustainable chemical plants. The most known process to separate azeotropes is extractive/azeotropic distillation. However, high pressures or high temperatures are required and therefore, a great amount of energy is necessary to reach a single fluid-phase system.

In the last decade, ionic liquids (ILs) have shown to possess the ability to act as extraction solvents and have been emerging as a greener alternative to organic solvents in the separation of azeotropes. Recently, high ionicity ionic liquids have been developed through the addition of inorganic salts to an ionic liquid and consequently, it has been showed that ionicity is particularly relevant in the effective separation of azeotropic mixtures.

In this work, the ionicity of three systems were studied and compared with the pure fluids, one composed of an ionic liquid + inorganic salt ([C_2MIM][SCN]+[NH_4][SCN]) and two composed of a mixture of two ionic liquids: 1-ethyl-3-methylimidazolium thiocyanate [C_2MIM][SCN] + 1-ethyl-3methylimidazolium ethyl sulfate [C_2MIM][C_2SO_4]; [C_2MIM][SCN] + 1-ethyl-methylimidazolium dicyanamide [C_2MIM][DCA]. Liquid-liquid equilibria for the two ternary systems: ethanol + heptane + ([C_2MIM][SCN], or [C_2MIM][SCN]+[C_2MIM][C_2SO_4]) was measured at 298.15K. Both the selectivity and the distribution coefficient were used in the assessment of the extraction solvent feasibility and a correlation of these parameters with ionicity was established.

Keywords Azeotropic mixture, Liquid-Liquid Equilibria, Ionicity, High Ionicity, Ionic Liquid, Extraction Efficiency

Contents

List of Figures

List of Tables

List of Abbreviations

[BMIM][$MeSO_4$]/ [C_4MIM][C_1SO_4]	1-buthyl-3-methylimidazolium methyl sulfate
[C_1MIM][C_1SO_4]	1-methyl-3-methylimidazolium methyl sulfate
[C_2MIM][C_1SO_4]	1-ethyl-3-methylimidazolium methyl sulfate
[C_2MIM][C_2SO_3]	1-ethyl-3-methylimidazolium sulfonate
[C_2MIM][C_2SO_4]/ [EMIM][$EtSO_4$]	1-ethyl-3-methylimidazolium ethyl sulfate
[C_2MIM][DCA]	1-ethyl-3-methylimidazolium dicyanamide
[C_2MIM][SCN]	1-ethyl-3-methylimidazolium thiocyanate
[Na][SCN]	Sodium thiocyanate
[NH_4][SCN]	Ammonium thiocyanate
BASIL	Biphasic Acid Scavenging utilising Ionic Liquids
IFP	Institut Français du Pétrole
ILs	Ionic liquids
IS	Inorganic salt
LLE	Liquid-Liquid Equilibria
PCC	Pearson Correlation Coefficient
ppm	parts per million
RMSD	Root-Mean-Square Deviation
VLE	Vapour-Liquid Equilibrium
HIIL	High Ionicity Ionic Liquid

List of Symbols

ρ	Density
η	Dynamic viscosity
f_m	Free molar volume
x	Molar fraction
R_m	Molar refraction
V_m	Molar volume
M_w	Molecular weight
n_D	Refractive index
w	Mass fraction
Λ_m	Molar conductivity
σ	Ionic conductivity
M_w	Molecular weight
V^E	Excess molar volume
β	Distribution coefficient
S	Selectivity

1. General Introduction

1.1 Azeotropes

Over the last decade, the scientific community has been paying more attention to novel processes based on greener technologies, due to the increasing concern about environmental issues, as well as the establishment of new regulations. In many areas of industry, solvent mixtures accumulate due to recycling difficulties. Their separation into pure components is necessary so that they can be reused. However, many of these solvent mixtures contain azeotropes, special mixtures whose separation has emerged as one of the "oldest" problems in chemical engineering.

The term *azeotrope* derives from the Greek words *a* – non, *zeo* - boil, *tropos* – way/mean, which basically means "no change when boiling"[1] and denotes a mixture of two or more components where the equilibrium vapour and liquid composition are equal at a given temperature and pressure. For this reason, azeotropes have actually been mistaken at times for single components because they boil at a constant temperature. The vapour has the same composition as the liquid and the azeotropoic mixture boils at a temperature other than that of the pure components' boiling points. Thus, the separation by conventional methods, such as simple distillation, is impossible. This is understood by the analysis of the vapour-liquid equilibrium (VLE) diagram, Figure 1.1 which shows a positive azeotrope or minimum-boiling mixtures (the boiling point of the azeotrope is lower than that of its pure components) of compounds X and Y. The region between the top and bottom trace indicates where the liquid and vapour phases exist simultaneously in equilibrium. If a mixture of, for example, 25% X+75% Y is heated up to a temperature AB, a vapour of composition B is generated with a corresponding liquid of composition A. If the vapour is cooled to point C, then the liquid obtained (distilled) is richer in X than it was at point A. This liquid can then be boiled and cooled successively, distilling a liquid that is richer and richer in X (point E), until the two curves meet. This point is called the azeotropic point and no matter how many times the liquid is boiled, the vapour and the liquid have the same composition, and one gets "stuck" with a distillate that contains the azeotropic composition, that won't change just by a simple boiling and cooling process.

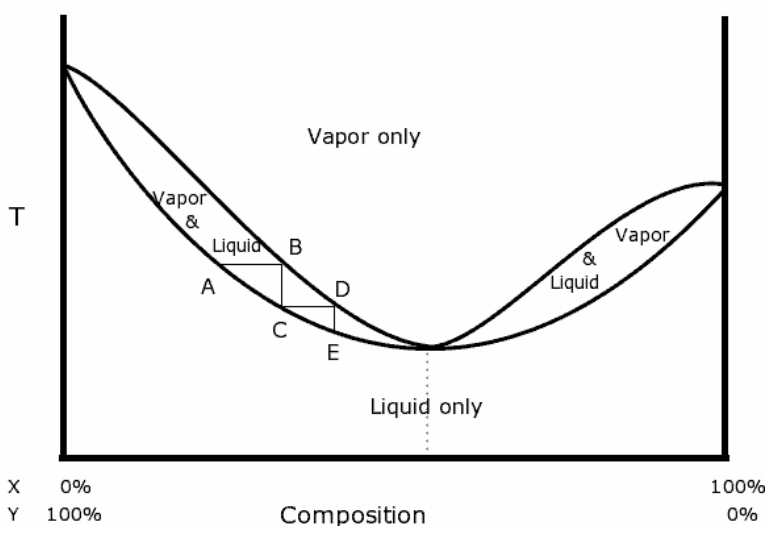

Figure 1.1 Temperature-composition VLE diagram of a positive azeotrope [2]

Negative azeotropes or maximum-boiling mixtures also exist, where the boiling point of the azeotropic mixture is higher than that of its pure components. In this case, if a mixture contains a composition very close to the azeotropic point, the distillate will always be further from the azeotrope than the original liquid mixture, whether a point was chosen on the right or the left of the azeotrope. Either way, no amount of distillation can make the distillate or the residue arrive on the opposite side of the diagram.

Numerous potential processes used to remove the compounds of an azeotrope have come to light such as azeotropic distillation, extractive distillation and liquid-liquid extraction [3]. Extractive distillation is the most common technique for removing one of the mixture components at or close to its azeotropic point. It involves the addition of a new heavy chemical compound (entrainer) which interacts with the components by altering their relative volatilities. Azeotropic distillation also involves the addition of a new compound but unlike the extractive distillation, both the entrainer and the components of the mixture must be vaporized. This way, if the entrainer is an ionic liquid, this type of distillation cannot be used, as its vapour pressure is negligible. The third component forms a ternary azeotrope and increases the volatility of the substances to be separated. Extractive distillation is generally more attractive, from the economical point of view because less entrainer is needed and less energy consumption is present. On the other hand, liquid-liquid extraction takes place at room temperature and atmospheric pressure and therefore, economic issues related to the energy consumed due to vaporization do not exist. This separation is based on the differences in miscibility between the involved components of the system.

1.2 Ionic Liquids

Ionic Liquids (ILs) are salts in which the ions are poorly coordinated, resulting in the existence of a liquid state below 100°C, or even at room temperature. They have been recognized for about a century, but have only started receiving closer attention in the last twenty years, having recently resulted in increasingly popular ‘‘green’’ media for engineers[4,5] due to their amazing physicochemical properties as well as their recyclability. Furthermore, IL scan be tailored for specific applications by accurately selecting the chemical nature of both the cation and the anion [6]. This fact, combined with the vast number of possible combinations of cation and anion, has conferred upon them the designation of ‘‘designer solvents’’. This feature is very attractive for chemical engineers since the fine-tuning of solvent properties permits the optimization process efficiency and cost. ILs were generally believed to be non-volatile, non-flammable thermally, and chemically stable salts but based on recent data, these vast assumptions have been progressively reconsidered for some families of ILs [7,8]. The toxicity of ILs is also a new issue that is driving the search for new environmentally friendly alternatives[9]. It is now accepted that the label ‘‘green solvents’’ does not apply to all ILs in all situations. Nevertheless, a widespread of IL applications regularly provides either superior yields or lower toxicities than conventional processes.

ILs have been studied as solvents in other applications that do not necessarily involve separation processes. They have been known to possess the ability of participating in catalysis such as transition-metal-metal catalysis [10]. An interesting example is the variety of ILs shown as potential solvents for isolating catalysts in alkene hydrogenation reactions; for instance, [EMIM][SbF6] and [EMIM][PF6] were tested in isolating the catalyst used in the hydrogenation of pent-1-ene. For both ILs the hydrogenation rates are significantly greater than seen for the same catalyst in acetone, presumably due to the stabilization of the transition-metal complex intermediate. [10]

1.3 Ionic liquids in the chemical industry

Ionic liquids are intrinsically outstanding candidates for industrial applications compared to volatile organic solvents. Organic solvents have been known for several centuries, and evidently occupy most of the solvent market in industry. However, if the properties of ILs and organic solvents are to be compared (see Table 1.1) [11], it could be anticipated that industry may be a natural environment for ILs. Since a lot of properties of ILs have yet to be discovered, at the current level of development they can nicely complement, and even sometimes work better than, organic solvents in a number of industrial processes.

Table 1.1 Comparison of organic solvents with ILs [a]

Property	**Organic solvents**	**ILs**
Number of solvents	>1000	>1,000,000
Applicability	Single function	Multifunction
Catalytic ability	Rare	Common and tuneable
Chirality	Rare	Common and tuneable
Vapour pressure	Obeys the Clausius–Clapeyron equation	Negligible vapour pressure under normal conditions
Flammability	Usually flammable	Usually non-flammable
Solvation	Weakly solvating	Strongly solvating
Polarity	Conventional polarity concepts apply	Polarity concept questionable
Tuneability	Limited range of solvents available	Virtually unlimited range means ‘‘designer solvents’’
Cost	Normally cheap	Typically between 2 and 100 times the cost of organic solvents
Recyclability	Green imperative	Economic imperative
Viscosity/cP	0.2–100	22–40,000
Density/g cm^{-3}	0.6–1.7	0.8–3.3
Refractive index	1.3–1.6	1.5–2.2

[a] The data summarised in this Table are not comprehensive, nor do they represent outliers; they are meant to give a brief visual comparison of typical values.

There are about 600 conventional solvents used in industry and at least 1 million (10^6) simple ILs that can easily be prepared in the laboratory. However, that total is just for simple binary systems. At the moment, only about 300 ILs are commercialised, so one can imagine how many opportunities in this field are still undiscovered and why this field of chemistry is so tempting[11].

Of all the industrial giants, BASF has done the most publicly to implement ILs technology. They possess the largest patent portfolio, have the broadest range of applications, and work openly with leading academics[11]. Probably, currently, the most successful example of an industrial process using ionic liquid technology is the BASIL (Biphasic Acid Scavenging utilising ILs) process[11]. It is used for the production of the generic photoinitiator precursor alkoxyphenylphosphines. In the original process, triethylamine was used to scavenge the acid that was formed in the course of the reaction, but this made the reaction mixture difficult to handle as the waste by-product, triethylammonium chloride formed a dense insoluble paste. Replacing triethylamine with 1-methylimidazolium results in the formation of 1-methylimidazolium chloride, an ionic liquid, which separates out of the reaction mixture as a discrete phase. The reaction is now carried out at a multi-ton scale, proving that handling large quantities of ILs is practical.

ILs as entrainers, or separation enhancers, [12] have been used to break common azeotropes, such as water–ethanol and water–tetrahydrofuran. The costs of separation and recycling of the entrainer are significantly reduced.

IFP (Institut Français du Pétrole) was the first to operate an ionic liquid pilot plant[13]. The Dimersol process, based on traditional technology, consists of the dimerisation of alkenes, typically propene (Dimersol-G) and butenes (Dimersol-X) to the more valuable branched hexenes and octenes[14]. The dimerisation reaction is catalysed by a cationic nickel complex and is commonly operated without solvent. The use of chloroaluminate(III) ILs as solvents for these

nickel-catalysed dimerisation reactions has been developed. The activity of the catalyst is much higher than in both solvent-free and conventional solvent systems, and the selectivity for desirable dimers is enhanced[11].

1.4 Ionic Liquid Mixtures

As previously referred, some ILs have long been held to be designer solvents, based upon the ability to independently vary their cations and anions. The possibility of fine-tuning can lead to an optimum solvent for a given application. This designer solvent concept has led to intense study of how changing ILs ions can affect their physico-chemical properties. As extensive as the ability to design ILs by selection of cations and anions is, there have been recent attempts to further develop this idea by using mixtures of ILs[15].

It is important to acknowledge the understanding of thermodynamics that is behind an IL when exploring the possibility of using it in a certain process and mixtures of ILs are not an exception. One of the most relevant aspects regarding ionic liquid mixtures from a thermodynamical point of view is its classification as an ideal mixture. The concept, in its most simple form, of an ideal mixture comes from the observation that at a given temperature the ratio of partial vapour pressure of a certain component above a liquid mixture to its vapour pressure as a pure liquid is approximately equal to its mole fraction in the liquid mixture. This is defined as Raoult's Law and liquid mixtures that obey it precisely are ideal solutions. Binary mixing leads to a mixture of liquid components in which all the changes in the energies of the intermolecular, or in case of ILs, interionic, interactions cancel each other out[15].

The belief that all properties of an ideal solution should always change in a linear manner with changing composition has been a common mistake. Only those properties of an ideal solution that are directly thermodynamically related to Raoult's Law must be a linear function of the mole fraction of the component, other may not necessarily be so. An example is that spectroscopic properties are often non-linear in ideal mixtures[15]. When linear behaviour would be expected for ideal behaviour, deviation from the expected value is defined as the *excess function*, *e.g.*, the difference between the experimental volume of mixing and the ideal volume of mixing is the excess volume of mixing, V^E, which can show both positive and negative values. The definition of ideal mixing also leads to $V^E = 0$. Hence, one should expect a linear change in the molar volume as the composition of the mixture changes between the two pure components. Molar volumes and, therefore, densities of mixtures are directly related to chemical potentials. Thus, molar volumes are expected to be a linear function of the mole composition of the components. Some caution does need to be applied to these measurements, because deviations from ideality in data generated by mixing liquids with very similar densities, as is often the case for ILs, can be obscured by the narrow data range.

It is likely that the application of ionic liquid mixtures as solvents for chemical synthesis is true, as is the case of ILs. The use of mixtures of ILs for catalysis as, for example, for ruthenium catalysed hydroformylation reactions in mixtures of $[C_4C_1im][NTf_2]$ and $[C_4C_1im]Cl$ showed increasing conversion rates with decreasing chloride-based IL concentrations indicating higher reactivity due to better solubility of the reactants[16]. Their use as battery electrolytes is another potential application of ionic liquid mixtures. The addition of lithium salts to ILs in battery applications has been found to extend their electrochemical window[17].

1.5 Azeotrope separation using Ionic Liquids

Azeotropes are involved in common chemical processes, including the production of methyl acetate, isopropanol and vinyl acetate. Additionally, due to their growing popularity, biofuel processes typically produce fermented products that form azeotropes with water, which is abundant in the fermentator. Among those products, ethanol is the most important example, due to its excellent properties as alternative fuel[3].

The remarkable azeotrope-breaking ability of ILs, their almost null volatility at room temperature[18] and their recovery and recycling ease, have allowed the recognition as possible alternatives to traditional solvents, such as sulfolane and tetraethylene glycol. Moreover, the physical and corrosion properties of ILs are generally more suitable for separation processes than those of inorganic molten salts, allowing the consideration of their use in azeotropic separation processes. Figure 1.2 maps the numerous publications already available on this subject presenting the distinct azeotropes studied with different IL anions and cations used as separating agents[3].

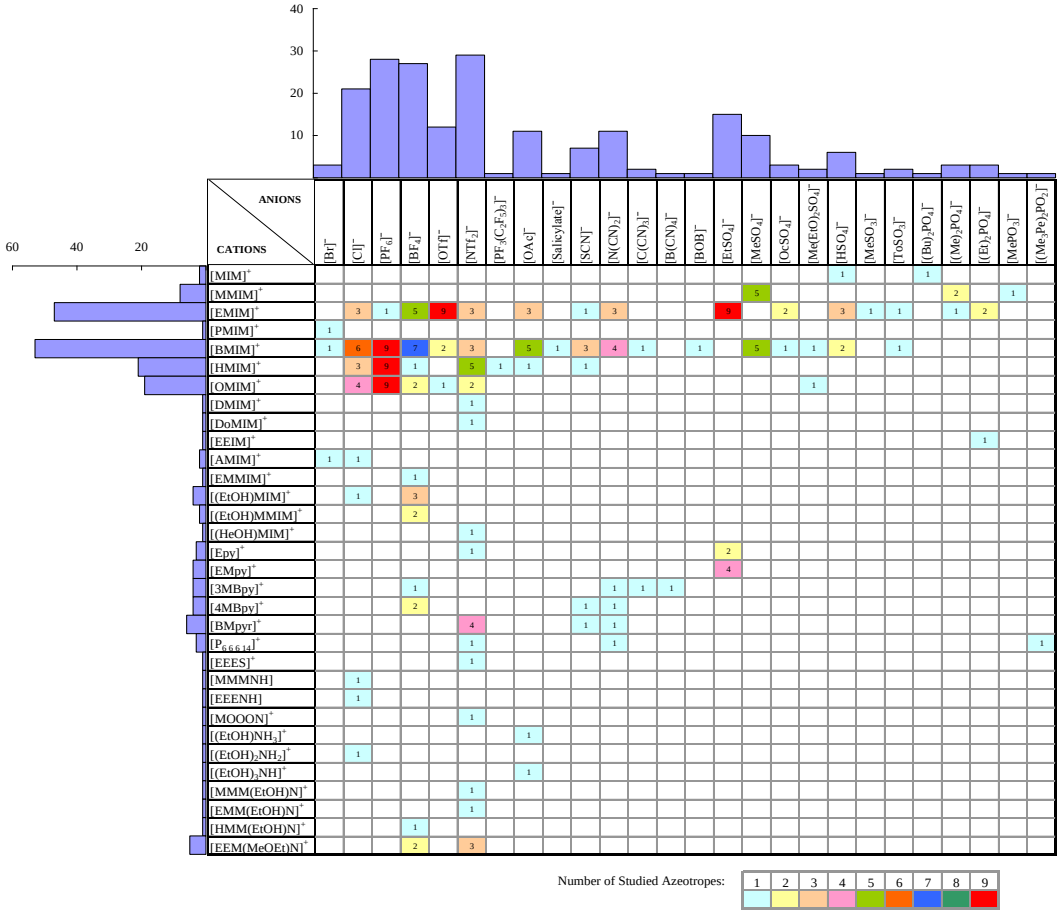

Figure 1.2 Mapping of azeotropes in the matrix of ILs anions and cations used as separating agents. The colours refer to the number of different studied azeotropes from literature per ion combination; the length of the bars gives the count per ion. [3]

ILs have demonstrated their high separation efficiency in breaking azeotropes including outstanding examples such as ethanol + water, aromatic + aliphatic mixtures and alcohol + alkane mixtures[19].

To be able to overcome the issue of azeotrope-breaking is relevant to the chemical industry, particularly to petrochemistry, as these industries often face the presence of close-

boiling mixtures due to the growth in the production of oxygenated additives in petrol. Alkanes and alcohols co-exist to produce these additives and the separation of these azeotropic systems is necessary so that the separated parts can be re-used in production cycles. The ethanol + heptane system is typically present in this production, where the process is created in order to achieve the reduction of lead in gasoline[20, 21].

The liquid–liquid separation leads to an environmentally friendly extraction process of these azeotropes as an alternative to the more common processes such as azeotropic distillation[22], pervaporation [23] and reverse osmosis[24]. Table 1.2 [25-33] evaluates IL azeotrope breakers for alkanols + alkanes[3]. Figure 1.3 compares alcohol/alkane selectivity values for the studied ternary systems for the ILs listed in Table 1.2 [3]. It can be concluded that a short alkyl side chain on the imidazolium cation increases selectivity, favouring ethanol/alkane separation. Based on the analysis of the ILs extraction capacities for ethanol + alkanes (hexane or heptane) systems, ILs with the methyl sulfate anion ($[C_1MIM][C_1SO_4]$ and $[C_2MIM][C_1SO_4]$) were included in a lab-scale extraction process incorporating a solvent recycling stage [28,29,31,32,33]. These selectivities are the highest reported in the literature for azeotropic separation in general using liquid-liquid extraction. The liquid-liquid equilibria data allowed researchers to identify theoretically appropriate operating conditions for countercurrent continuous extraction process at room temperature including a solvent recycling stage. Simulation techniques were then used to optimize operational conditions. Experiments with a laboratory-scale packed column under steady-state conditions achieved a raffinate purity of over 98 wt %.

Table 1.2 Azeotropes in the literature regarding the separation of alcohols + alkanes. ILs used as azeotrope breakers. Alcohol/alkane selectivity from LLE data (S^{LLE}) at 0.01 alcohol molar fraction in organic phase. [3]

Azeotrope	ILs	S^{LLE}	Remarks	Reference
Methanol + Heptane	[OMIM][Cl]	401.0	LLE data at 298.15 K	[25]
Ethanol + Hexane	$[EMIM][EtSO_4]$	3631	LLE data at 298.15 K	[26]
	$[HMM(EtOH)N][BF_4]$	1584	LLE data at 298.15 K	[27]
	$[BMIM][MeSO_4]$	482.1	LLE data at 298.15 K	[28]
	$[MMIM][MeSO_4]$	9427	LLE data at 298.15 K	[29]
	$[HMIM][PF_6]$	330.7	LLE data at 298.15 K	[30]
	$[OMIM][PF_6]$	115.2		
Ethanol + Heptane	$[EMIM][EtSO_4]$	2343	LLE data at 298.15 K	[26]
	$[MMIM][MeSO_4]$	5592	LLE data at 298.15 K	[31]
	$[OMIM][PF_6]$	229.8	LLE data at 298.15 K	[30]
	$[BMIM][MeSO_4]$	22326	LLE data at 298.15 K	[32]
	$[HMIM][PF_6]$	2861	LLE data at 298.15 K	[33]
	[OMIM][Cl]	457.0	LLE data at 298.15 K	[25]

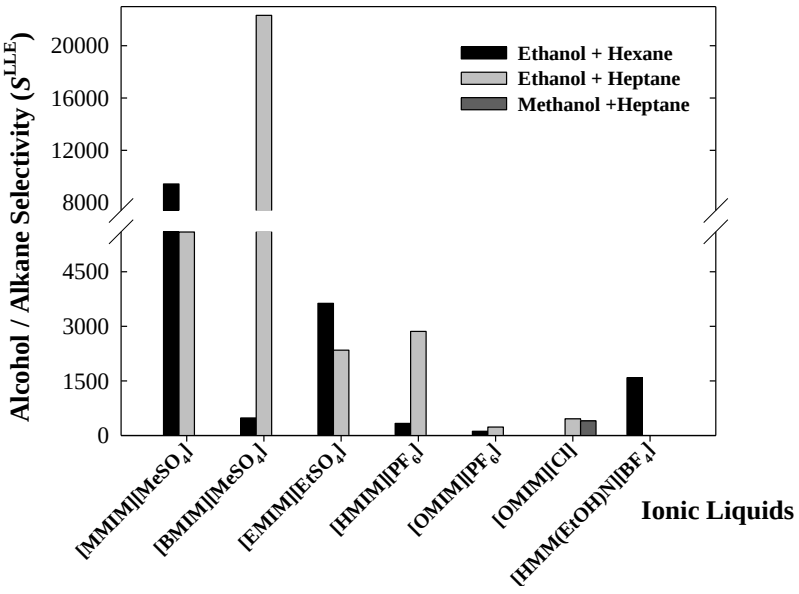

Figure 1.3 Alcohol/alkane selectivity versus ILs [25-33] used in the separation of the alcohols + alkanes systems at 298.15 K and alcohol molar fraction in organic phase ≈ 0.01. [3]

ILs based on the alkyl sulfate anion show the greatest potential as solvents in separation by liquid-liquid extraction of the two azeotropes reviewed. $[C_2MIM][C_2SO_4]$ is the most frequently studied (Figure 1.2) in this extraction process. Figure 1.4 compares $[C_2MIM][C_2SO_4]$ selectivities for different azeotropes separated by liquid-liquid extraction[3]. The best results were obtained for the separation of ethanol with heptane or hexane. From the data presented in Figure 1.3 and Table 1.2, it can be concluded that $[C_1MIM][C_1SO_4]$ shows better results than $[C_2MIM][C_2SO_4]$ and $[C_4MIM][C_1SO_4]$.

$[C_1MIM][C_1SO_4]$ and $[C_4MIM][C_1SO_4]$ were used as azeotrope breakers in a laboratory-scale liquid-liquid extraction process and the results also confirmed that $[C_1MIM][C_1SO_4]$ has the highest extraction efficiency [32,33,30,34]. These papers confirm the assumption that the IL regeneration and recycling are indeed simple for this process, which is a great advantage relative to traditional extraction solvents.

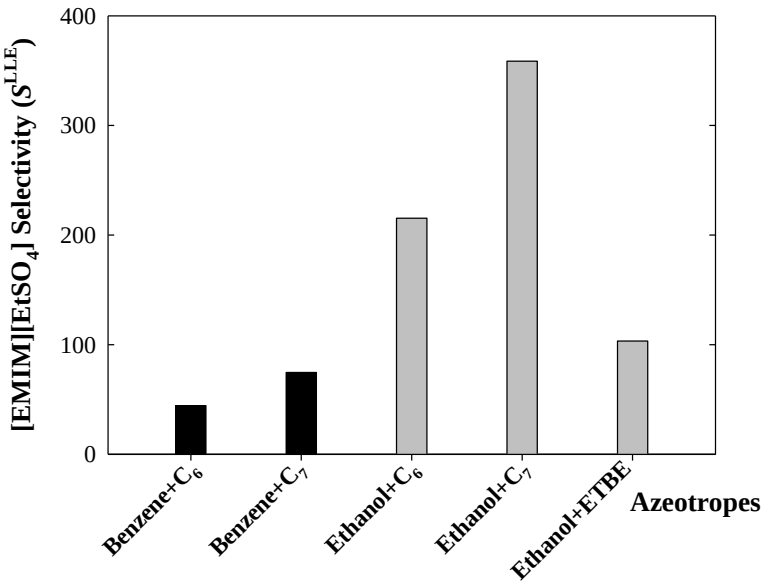

Figure 1.4 [EMIM][$EtSO_4$] selectivity (S^{LLE}) for several azeotropes separated by liquid-liquid extraction [30,42,43] at 298.15 K and solute molar fraction in organic phase ≈ 0.05. [3]

1.6 Ionicity in Ionic Liquids

Over the past ten years, the concept of ionicity of ILs has been debated by several authors and it was shown that a quantitative description of the ionicity allows an important understanding of the thermodynamic and thermophysical behaviour of ILs[35]. The simplest concept of ionicity is based on a relationship between the fluidity and the capability of the ions present to move from one site to another, experimentally determined by the ionic conductivity. The measurement of the ionicity is determined by the classical Walden rule, in which the conductivity per mole of substance is inversely proportional to its viscosity[36]. These two properties are directly related to the occurrence of ion pairs, the formation of aggregates and the existence of ionic networks. A classification diagram for ionic liquid based on the classical Walden rule and a Walden plot will be illustrated and explained in Chapter 2. Basically, the closer the experimental points are to the "ideal" line, which is the straight line that passes through the origin, the higher the ionicity.

Previous work established that some ionic liquid's ionicity could be improved by the dissolution of simple inorganic salts (IS) in their milieu[37]. The increase in Coloumbic interactions in the complex nature of ILs could be behind the explanation of this improvement, while preserving the liquid nature of the new ionic media.

In addition to the study of dissolving an IS with an IL, the mixing of two IL is also of particular interest in developing High Ionicity ILs. The capability of subtly changing the chemical structure of the anion and cation (also referred to as fine-tuning) is one of the most appealing characteristics of ILs. Mixtures of ILs increase this specificity due to the wide combinations and possible applications that arise from mixing two or more ILs.

1.7 Objectives

The objective of this dissertation was to verify a possible connection between the effectiveness of extracting ethanol from its azeotropic mixture with heptane and the use of a solvent with a greater ionicity.

Three systems were studied to analyse how alternating the anion and maintaining a common cation affects the ionicity. The IL/IS system studied was 1-ethyl-3-methylimidazloium thiocyanate [C_2MIM][SCN] combined with ammonium thiocyanate ([NH_4][SCN]). The remaining systems were 1-ethyl-3-methylimidazolium thiocyanate [C_2MIM][SCN] mixed with 1-ethyl-3-methylimidazoilum ethyl sulfate/dicyanamide ([C_2MIM][C_2SO_4], [C_2MIM][DCA]).

ILs based on the thiocyanate and dicyanamide anions are already known to present a high conductivity in comparison to other ILs with different anions, not to mention their low viscosity and density, which was why they were chosen to be part of this study. The ammonium based salt was chosen to give continuation to previous studies[38] where this salt was dissolved in ILs with different anions than thiocyanate, as well as the fact that the cation NH_4^+ is perfectly capable of establishing hydrogen bonds and interacting easily with the anion, resulting in high solubilites in the ionic liquid in comparison to other cations studied such as Na^+.

2. Thermophysical Characterisation of Ionic Liquids

2.1 Introduction

The quantification and understanding of the ionicity of ILs is of much interest as not all ions present in ILs appear to be available to participate in conduction processes. Naturally, some level of ionic conductivity is to be expected of all ILs, but interestingly, some exhibit much lower conductivity than others even after differences in viscosity are allowed for. This is to be expected of ionic media in which ion pairs and formation of aggregates may strongly influence conductivity. These effects are of interest in applications of ILs as electrolytes in electrochemistry and electrochemical devices, such as lithium batteries. The understanding of the factors that influence the conductivity effects is of importance as their impact spreads beyond the electrochemistry to their solvent properties and vapour pressure, which are predominantly related to this dissertation. Hence, the question "how ionic is an ionic liquid?" becomes of quite significance[36].

A qualitative approached to this question was described by Angell and co-workers[39-41]

based on the Walden rule, which establishes a relationship between the molar conductivity (Λ_m) and the viscosity (η), two properties that are directly related to the occurrence of ion pairs, the formation of aggregates and the existence of ionic networks:

$$\boldsymbol{\Lambda_m \eta = c} \qquad \textbf{(2.1)}$$

where, c is a temperature dependent constant. On a plot of $\log(\Lambda_m)\ vs\ \log(\eta^{-1})$ this rule predicts a straight line that passes through the origin; this representation has become known as a "Walden plot". Data for a 0.01M KCl solution provide a suitable calibration reference line[41] on the Walden plot as shown in Figure. 2.1. Data from a variety of electrolytes can then be placed on the Walden plot, including any ionic liquid for which viscosity and conductivity measurements are available. Most ILs fall below the line, more or less so depending on their structure.

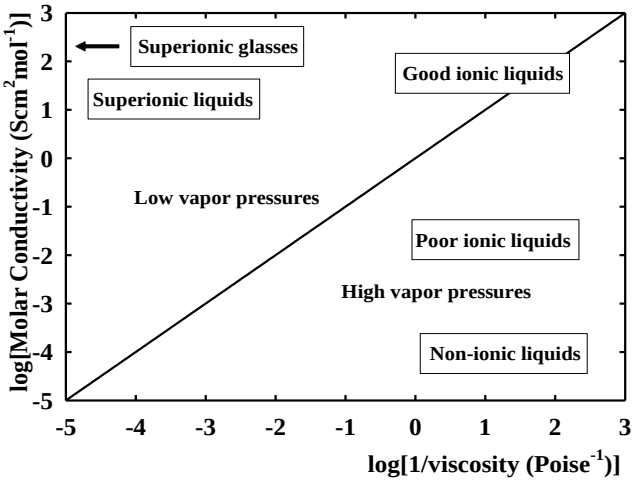

Figure 2.1 Classification diagram for ILs based on the classical Walden rule and a Walden plot

The first studies of solubilising simple inorganic salts in ILs focused on the development of systems for lithium batteries where it was thought that dissolving lithium in an ionic liquid could lead to an increase in conductivity[44-46]. Only later on was the effect of the addition of ISs on the ionicity of ILs explored. This act has already shown that the ionicity of the pure ionic liquid can be improved. The study of solubilizing ammonium thiocyanate $[NH_4][SCN]$ in 1-ethyl-3-methylimidazolium ethyl sulfate $[C_2MIM][C_2SO_4]$ [37] or in 1-ethyl-3-methylimidazolium sulfonate $[C_2MIM][C_2SO_3]$ [35] is a successful example of this statement.

In this thesis, a similar study was carried out, where the same salt was dissolved in 1-Ethyl-3-methylimidazolium thiocyanate $[C_2MIM][SCN]$ to verify a possible increase in ionicity in comparison to the pure ionic liquid. The thiocyanate-based ionic liquid was chosen due to its appealing thermodynamic properties, such as low viscosity and density and high conductivity compared with most ILs. Moreover, the fact that this ionic liquid is not yet studied, rouse a greater interest in its use.

The study of the solubility of the salt in the ionic liquid is of great importance since all binary mixtures need to be prepared within the solubility range in order to conduct a study of the ionicity. Also, very different solubility limits have been found for different inorganic salts in different ILs[38]. Therefore, a simple visual detection method was used to determine the solubility of the $[NH_4][SCN]$ in $[C_2MIM][SCN]$. Literature showed that at a molar fraction of 0.1729 the salt is soluble[38] in the ionic liquid. In this work, using a visual detection method, it was observed that a molar fraction of 0.2594 of the salt showed insolubility. A screening of the solubility of sodium thiocyanate [Na][SCN] in $[C_2MIM][SCN]$ was also conducted and compared with that of the ammonium thiocyanate in the same IL. Nevertheless, the option of using $[NH_4][SCN]$ in $[C_2MIM][SCN]$ was made in order to compare and to give continuation of previous studies, where this salt was solubilized in $[C_2MIM][C_2SO_4]$ and the increase in ionicity was demonstrated.

In addition to the study of dissolving an IS with an IL, the mixing of two ILs was also considered in the development of an ionic media with high ionicity. As discussed in Chapter 1, the capability of tuning the chemical structure of the anion and cation is one of the most interesting characteristics of ILs and mixing them increases this specificity due to the vast possible combinations. Thus, mixing 1-ethyl-3-methylimidazolium thiocyanate $[C_2MIM][SCN]$

with 1-ethyl-3-methylimidazoilum ethyl sulfate [C_2MIM][C_2SO_4] took place in this study. The former was also mixed with 1-ethyl-3-methylimidazolium dicyanamide [C_2MIM][DCA].

This chapter goes on to the thermophysical and thermodynamic characterization of the ILs and their mixtures with either an inorganic salts or another ionic liquid mentioned above in order to fulfil the objectives of this dissertation. This implies the measurement of densities, viscosities and ionic conductivities of all three systems: ([C_2MIM][SCN] + {[NH_4][SCN], [C_2MIM][DCA] and [C_2MIM][C_2SO_4]}).

2.2 Materials and Experimental Procedure

2.2.1 Materials

The chemical structure of all ILs and inorganic salts used in this work are illustrated in Table 2.1 including their source and purity. In order to reduce the water and other volatile substances contents, a moderately high temperature (50 ºC) and vacuum (10^{-3} kPa) was applied to all samples for at least 48 h prior to their use. The final mass fraction of water was measured by Karl Fischer coulometric titration. All dried ILs and mixtures contained 900-1100 ppm of water.

Table 2.1 Name, abbreviation, chemical structure and supplier and purity of all chemicals used

Formal name, abbreviation	Chemical Structure	Supplier and purity (%)
ILs		
1-Ethyl-3-methylimidazolium thiocyanate, [C_2MIM][SCN]	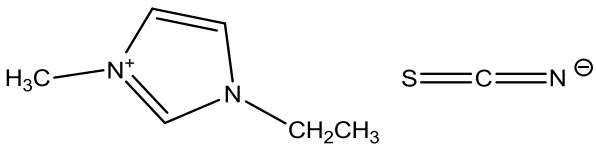	Fluka, 95 %
1-Ethyl-3-methylimidazolium ethyl sulfate [C_2MIM][C_2SO_4]	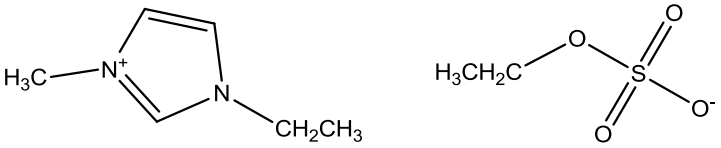	Iolitec, 98 %
1-Ethyl-3-methylimidazolium dicyanamide [C_2MIM][DCA]	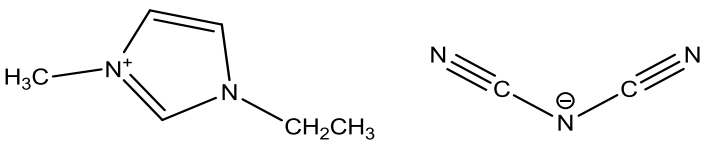	Iolitec, 98 %
Inorganic Salts		
Ammonium Thiocyanate [NH_4][SCN]	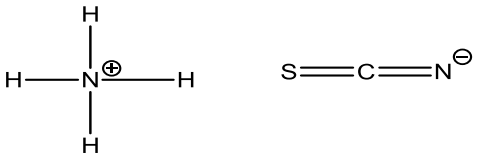	Sigma-Aldrich, 97.5 %

2.2.1 Experimental procedure

2.2.1.1 Viscosity and density measurements

Viscosity and density were measured in the temperature range between 298.15 and 353.15 K at atmospheric pressure using an automated SVM 3000 Anton Paar rotational Stabinger viscometer–densimeter (Figure 2.2.). The SVM 3000 uses Peltier elements for fast and efficient thermostability. The temperature uncertainty is ± 0.02 K. The precision of the dynamic viscosity measurements is ± 0.5 % and the absolute uncertainty of the density is ± 0.0005 g.cm^{-3}. The overall uncertainty of the viscosity measurements (taking into account the purity and handling of the samples) is estimated to be 2 %. Triplicates were measured and the reported result is the average value.

Figure 2.2 SVM 3000 Anton Paar rotational Stabinger viscometer-densimeter

2.2.1.2 Refractive index measurements

The refractive indices were measured at atmospheric pressure and in the temperature range between 298.15 and 353.15 K through an automated Anton Paar Refractometer Abbemat 500 (Figure 2.3) with a precision of $\pm$ 5.10^{-5}. Triplicates were measured and the reported result is the average value. The absolute uncertainty of the refractive indices was$\pm$0.00005.

Figure 2.3 Anton Paar Refractometer Abbemat 500

2.2.1.3 Ionic Conductivity measurements

The ionic conductivities were measured using a CDM210 Radiometer Analytical conductivity meter (Figure 2.4). They were performed in a jacketed glass cell containing a magnetic stirrer and temperature regulated circulating water from a bath controlled to ± 0.01K. The temperature in the cell was measured by means of a platinum resistance thermometer coupled to a Keithley 199 System DMM/Scanner. The thermometer was calibrated with high–accuracy mercury thermometers (0.01 K). For the ionic conductivity measurements, about 1.5 ml of the sample was added to the thermostatic cell and vigorously stirred. The cell was closed with screw caps to ensure a secure seal and flushed with dry nitrogen to prevent humidity. Each single measurement was performed as quickly as possible to minimize undesired effects (such as self–heating of the samples, ionization in the electrodes, etc) that might modify the measured conductivity values. This conductivity meter uses an alternating current of 12 V and 2.93–23.4 kHz of frequency in the range of conductivities measured in this work. The use of high frequency alternating current (greater than 600Hz) and the fact that the electrodes were platinised avoided the polarization phenomena that can occur at the surface of the cell electrodes. The meter had been previously calibrated at each temperature with certified 0.01 D and 0.1 D KCl standard solutions supplied by Radiometer Analytical. This technique was validated using the pure ILs 1-Ethyl-3-methylimidazolium ethyl sulfate ($[C_2MIM][C_2SO_4]$) and 1-Ethyl-3-methylimidazolium thiocyanate ($[C_2MIM][SCN]$). The obtained results were compared with the published data showing a maximum relative deviation of 2 %. Every conductivity value was determined twice to ensure its reproducibility within 1 % in absolute value.

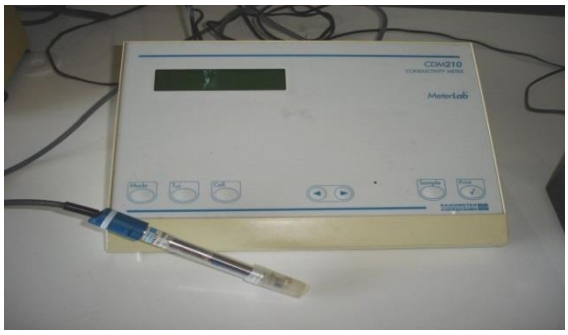

Figure 2.4 CDM210 Radiometer analytical conductivity meter

2.3 Results and Discussion

2.3.1 Thermophysical and thermodynamic properties for [C_2MIM][SCN] + [NH_4][SCN]

2.3.1.1 Density and viscosity

The measured density and viscosity data for the binary mixture [C_2MIM][SCN] + [NH_4][SCN] as a function of inorganic salt molar fraction at different temperatures (298.15 to 353.15 K) are given in Table 2.2. These data are also found in Figure 2.5 and Figure 2.6, respectively as a function of ammonium thiocyanate molar composition.

Table 2.2 Density, ρ, and dynamic viscosity, η for the binary system [C_2MIM][SCN] (1) + [NH_4][SCN](2) at several temperatures

x_2	ρ (g.cm^{-3})	η (mPa.s)	ρ (g.cm^{-3})	η (mPa.s)	ρ (g.cm^{-3})	η (mPa.s)
	298.15 K		**318.15 K**		**338.15 K**	
0	1.1156	23.062	1.1036	12.976	1.0919	8.297
0.0390	1.1158	25.912	1.1038	14.279	1.0920	9.010
0.0990	1.1168	29.912	1.1049	16.001	1.0934	9.900
0.1395	1.1160	31.581	1.1040	16.712	1.0926	10.241
	303.15 K		**323.15 K**		**343.15 K**	
0	1.1125	19.677	1.1006	11.488	1.0889	7.532
0.0390	1.1127	21.967	1.1009	12.592	1.0890	8.156
0.0990	1.1138	25.158	1.1020	14.027	1.0905	8.914
0.1395	1.1130	26.486	1.1012	14.615	1.0899	9.195

	308.15 K		328.15 K		348.15 K	
0	1.1095	16.972	1.0977	10.246	1.0858	6.869
0.0390	1.1097	18.843	1.0980	11.188	1.0859	7.423
0.0990	1.1108	21.400	1.0991	12.405	1.0876	8.076
0.1395	1.1100	22.473	1.0984	12.876	1.0871	8.317
	313.15 K		**333.15 K**		**353.15 K**	
0	1.1065	14.543	1.0948	9.019	1.0826	6.169
0.0390	1.1067	16.107	1.0950	9.852	1.0827	6.683
0.0990	1.1078	18.209	1.0962	10.923	1.0847	7.276
0.1395	1.1070	19.095	1.0955	11.332	1.0842	7.484

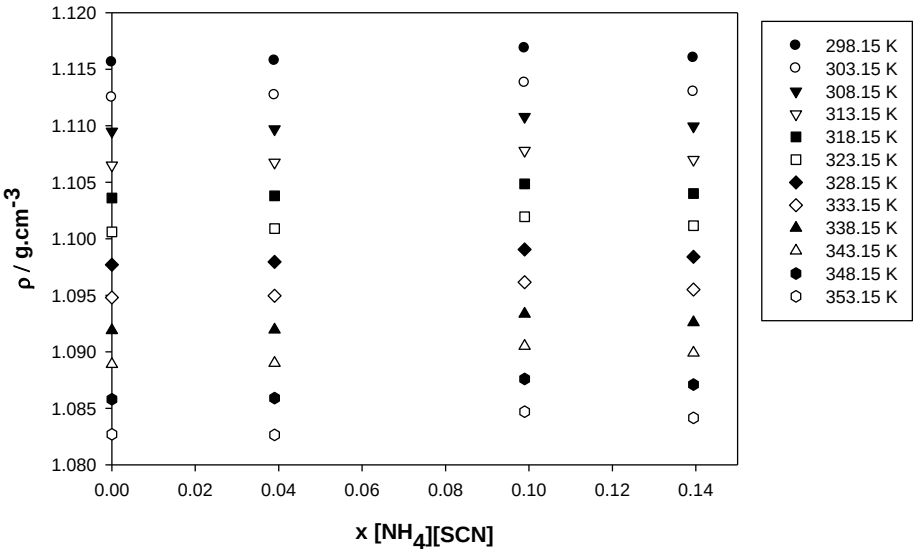

Figure 2.5 Density as a function of $[NH_4][SCN]$ concentration in the solubility range for the binary system $[C_2MIM][SCN] + [NH_4][SCN]$.

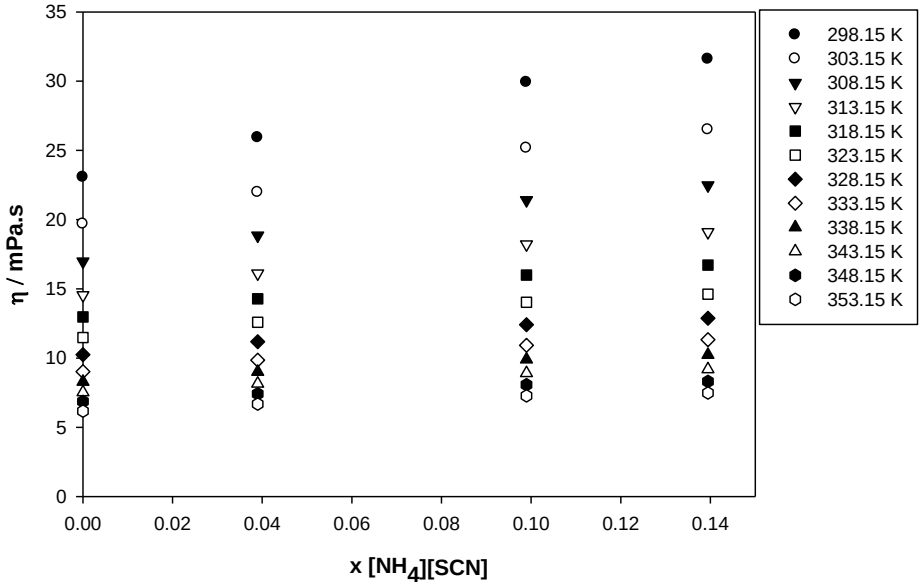

Figure 2.6 Dynamic viscosity as a function of $[NH_4][SCN]$ molar fraction in the solubility range for the binary system $[C_2MIM][SCN]$ + $[NH_4][SCN]$.

The measured density values for the binary mixtures $[C_2MIM][SCN]$ + $[NH_4][SCN]$ slightly increase with increasing $[NH_4][SCN]$ concentration. Due to the very low solubility limit of ammonium thiocyanate in the $[C_2MIM][SCN]$, in comparison with other ILs, such as $[C_2MIM][C_2SO_4]$, for which the solubility limit is $x[NH_4][SCN] \approx 0.5$ [37], only a small increase in density could be appreciated. Regarding viscosity, the value for this property clearly increased from the pure ionic liquid up to x $[NH_4][SCN] \approx 0.14$. It can be observed that both the density and viscosity of the pure ionic liquid are lower than the binary mixtures. This behaviour is completely different than that found for other binary mixtures of IL+IS, where the addition of salt decreased the density of the mixture[35]. Figure 2.7 and Figure 2.8 illustrate the temperature dependence of the density and viscosity, respectively, for the $[C_2MIM][SCN]$ + $[NH_4][SCN]$ mixture at a concentration of 0.1395 in molar fraction of inorganic salt, close to the solubility limit, and compares it with behaviour obtained for the pure ionic liquid $[C_2MIM][SCN]$.

The density values, ρ ($g.cm^{-3}$), are fitted as a function of temperature, T (K), by the method of the least squares using the linear expression given by Equation 2.2.

$$\boldsymbol{\rho = a + b\,T} \qquad \textbf{(2.2)}$$

where a and b are adjustable parameters which are listed in Table A.1 in Appendix A. Dynamic viscosities and conductivities were fitted as a function of temperature, using an Arrehnius-like law (Equation 2.3):

$$\ln(X) = \ln(X_0) - \frac{Ea}{RT} \qquad (2.3)$$

where X is the property, η/ (mPa.s) or σ/ (mS.cm^{-1}); X_0 is the pre-exponential factor (η_0 or σ_0); Ea is the activation energy; R the gas constant and T the temperature in Kelvin. The fitted parameters are listed in Table A.2 in Appendix A and a good adjustment of the properties as a function of temperature was made.

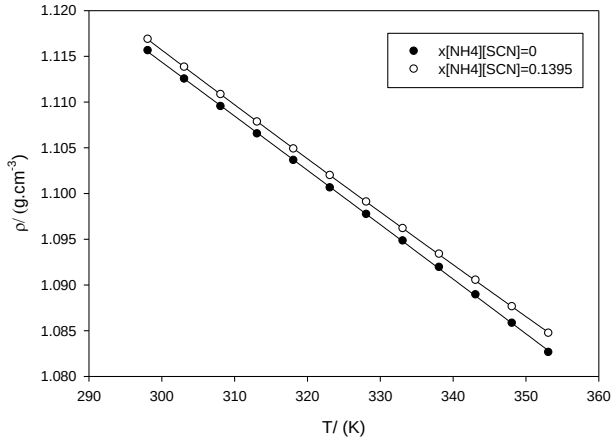

Figure 2.7 Density, ρ as a function of temperature for pure [C_2MIM][SCN] and [C_2MIM][SCN] + x [NH_4][SCN]=0.1395

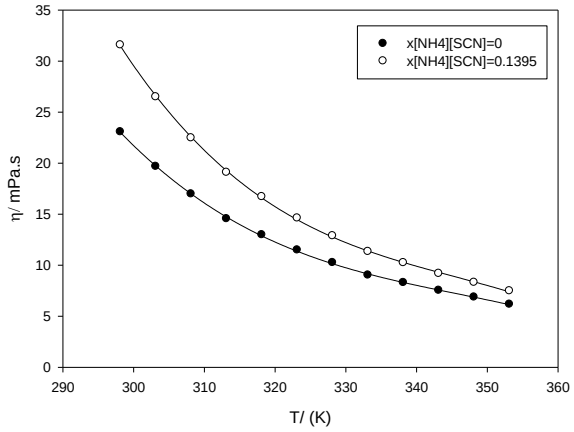

Figure 2.8 Viscosity, η as a function of temperature for pure [C_2MIM][SCN] and [C_2MIM][SCN] + x [NH_4][SCN]=0.1395

2.3.1.2 Refractive Index

The refractive indices for the system [C_2MIM][SCN] + [NH_4][SCN] are shown in Table 2.3, for the concentration range between 0 and 0.1395 mole fraction along with the molar volume, molar refraction, and free molar volume values. The addition of salt increased the refractive index of the mixture, and within the studied concentration range of [NH_4][SCN], this property decreased linearly with increasing temperature.

The Lorentz–Lorenz equation can be used to calculate the molar refraction or molar polarizability, R_m, which can be related both to density, ρ, and refractive index, n_D. (Equation 2.4)

$$R_m = \left(\frac{n_D^2-1}{n_D^2+2}\right) V_m \qquad \textbf{(2.4)}$$

where V_m is the molar volume. The molar refraction is considered as a measure of the hard-core volume of one molecule and it can be used to calculate the molar free volume, *f*m, of a solution, by Equation 2.5.

$$f_m = (V_m - R_m) \qquad \textbf{(2.5)}$$

The values for the calculated molar refractions (from Equation 2.4) and molar free volumes (from Equation 2.5) of all the studied samples are listed in Table 2.3 together with the molar volume calculated from density values. Figure 2.9 illustrates the molar free volumes for the neat ionic liquid [C_2MIM][SCN] and its binary mixture with [NH_4][SCN] at a concentration of 0.1395 in molar fraction of salt.

Table 2.3 Refractive indices, n_D, molar free volume, f_m, molar volume, V_m and molar polarizability, R_m for the binary system [C_2MIM][SCN] (1) + [NH_4][SCN] (2) at several temperatures.

x_2	n_D	V_m ($cm^3.mol^{-1}$)	R_m ($cm^3.mol^{-1}$)	f_m ($cm^3.mol^{-1}$)
		298.15 K		
0	1.548555	151.703	48.222	103.480
0.0390	1.548582	151.682	48.218	103.465
0.0990	1.550318	151.533	48.296	103.236
0.1395	1.550388	151.648	48.338	103.310
		303.15 K		
0	1.547538	152.125	48.282	103.843
0.0390	1.547224	152.098	48.251	103.847
0.0990	1.549275	151.948	48.353	103.595
0.1395	1.549011	152.057	48.368	103.689
		308.15 K		
0	1.545926	152.537	48.295	104.242
0.0390	1.545397	152.509	48.247	104.262
0.0990	1.547591	152.358	48.360	103.998
0.1395	1.547440	152.475	48.386	104.089
		313.15 K		
0	1.544204	152.950	48.299	104.652
0.0390	1.543562	152.916	48.240	104.675
0.0990	1.545913	152.771	48.368	104.403
0.1395	1.545526	152.881	48.374	104.904
		318.15 K		
0	1.542534	153.352	48.302	105.050
0.0390	1.541099	153.324	48.187	105.137
0.0990	1.544311	153.179	48.379	104.800
0.1395	1.544003	153.297	48.393	104.904
		323.15 K		
0	1.541057	153.770	48.324	105.446

0.0390	1.539412	153.728	48.189	105.540
0.0990	1.542763	153.582	48.391	105.191
0.1395	1.542402	153.693	48.400	105.294

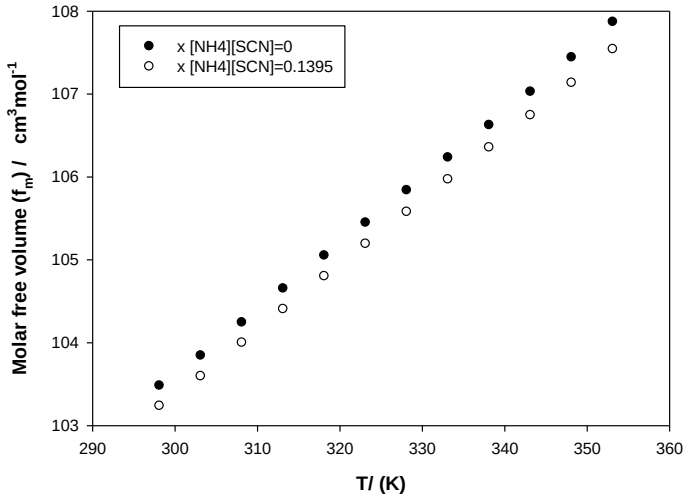

Figure 2.9 Molar free volume as a function of temperature for the pure $[C_2MIM][SCN]$ and for the mixture $[C_2MIM][SCN]$ + *x*$[NH_4][SCN]$=0.1395

It can be observed that the molar free volumes decrease with $[NH_4][SCN]$ concentration indicating the favourable interactions between the ions in the IL and the ions of the inorganic salt. Comparing the results obtained for the molar free volume of pure $[C_2MIM][SCN]$ and those published in the literature for the pure $[C_2MIM][C_2SO_4]$the $[C_2MIM][SCN]$ [35] has lower molar free volume in the whole range of temperature which means that it has less space available to accommodate $[NH_4][SCN]$ than $[C_2MIM][C_2SO_4]$. As expected the free volume increases with temperature, as also observed in literature.

The analysis of the molar free volumes can lead to important conclusions associated with the solubility of different species in a solvent. However, the mechanisms of solubilisation have other important contributions from enthalpy nature, thus related to the solvation of the solute in the solvent due to the establishment of interactions. Therefore, refractive data can be useful since they provide insights at the macroscopic level about the role of entropic factors in the solubilisation of an inorganic salt in an IL.

2.3.1.3 Ionic Conductivity

The evolution of the conductivity versus $[NH_4][SCN]$ concentration is plotted in Figure 2.10, and the data obtained appear in Table 2.4. The addition of ammonium thiocyanate caused a decrease in conductivity from the pure ionic liquid $[C_2MIM][SCN]$ up to x $[NH_4][SCN] \approx 0.1395$ due to a decrease in the effective mobility of the ionic carrier, that also results in an increase of viscosity.

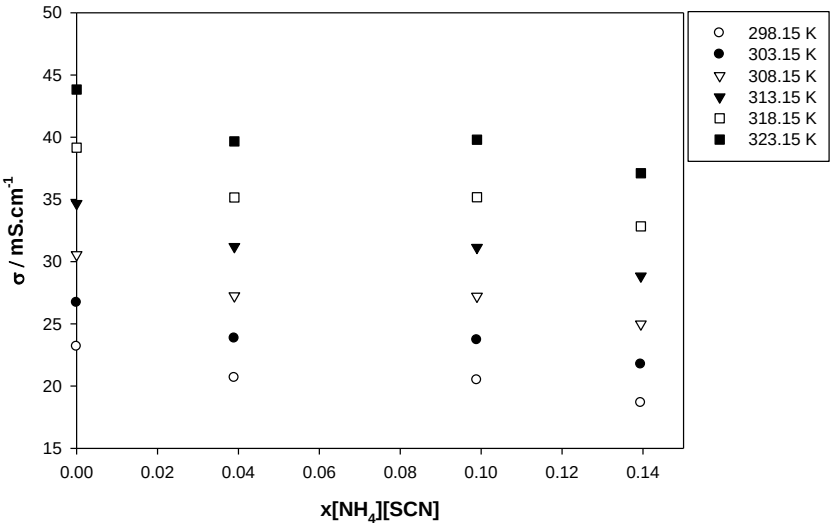

Figure 2.10 Ionic conductivity as a function of $[NH_4][SCN]$ concentration in solubility range for the binary system $[C_2MIM][SCN]+[NH_4][SCN]$

Table 2.4 Ionic conductivity, σ, for the binary system $[C_2MIM][SCN]$ (1) + $[NH_4][SCN]$ (2) at several temperatures

	σ/ (mS.cm^{-1})					
x_2	**298.15 K**	**303.15 K**	**308.15 K**	**313.15 K**	**318.15 K**	**323.15 K**
0	23.17	26.70	30.55	34.66	39.15	43.83
0.0390	20.66	23.84	27.24	31.21	35.16	39.66
0.0990	20.47	23.69	27.21	31.13	35.18	39.80
0.1395	18.65	21.74	24.98	28.83	32.84	37.10

2.3.1.4 Walden Plot

After the study of the thermodynamic and thermophysical properties, it was possible to determine the ionicity of the system, as, according, to the Walden rule, the ionicity is related to the viscosity and molar conductivity (Equation 2.6). The determination of the density of the system was necessary since the molar conductivity was calculated as:

$$\Lambda_m = \frac{\sigma}{\rho . M_W} \qquad \textbf{(2.6)}$$

with the σ conductivity in $S.cm^{-1}$, ρ the density in $g.cm^{-3}$ and M_W the molecular weight in $g.mol^{-1}$.

Using Equation 2.1 and 2.6 it was possible to provide the Walden plot for the system (Figure 2.11) which allowed the calculation of its ionicity by evaluating the Walden deviation, ΔW, (Figure 2.12), which is the distance between the "ideal" line and the experimental points, at a fixed fluidity. As mentioned before, the so-called ideal line represents the behaviour of an ideal electrolyte where complete dissociation is attained.

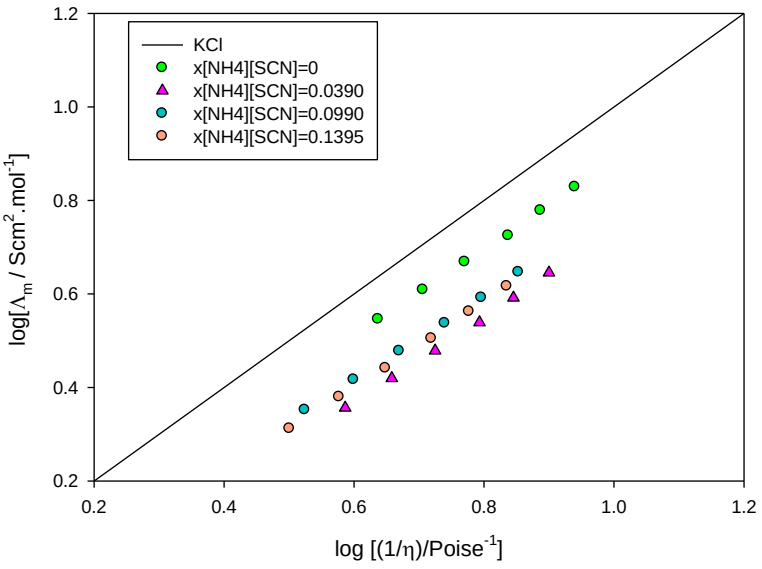

Figure 2.11 Walden plot for the binary system $[C_2MIM][SCN] + [NH_4][SCN]$ at different concentrations. At each concentration different temperatures at plotted.

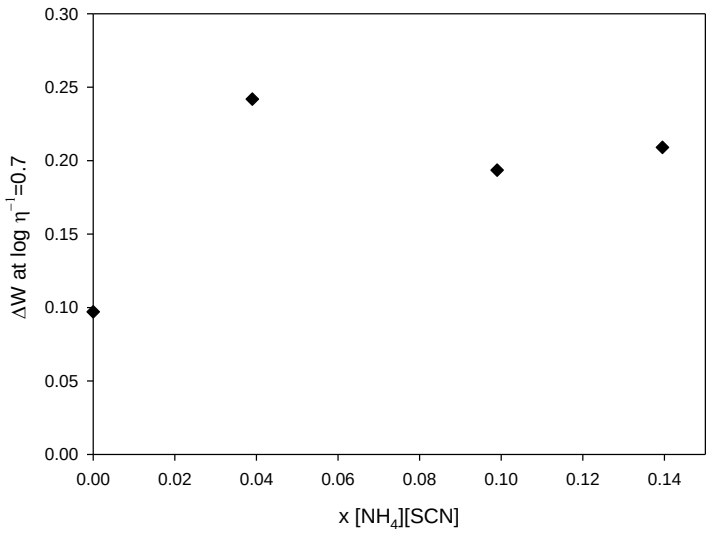

Figure 2.12 Deviation from the "ideal" Walden behaviour for the binary system $[C_2MIM][SCN]$ + $[NH_4][SCN]$ plotted against inorganic salt mole fraction.

It is possible to observe that the addition of the salt ammonium thiocyanate to the ionic liquid, did not increase the ionicity of the system, as the binary mixtures present a greater deviation from the "ideal" behaviour than the pure ionic liquid, for the whole solubility range. The difficulty of fully understanding why this happened leans on the fact that this study is based on macroscopic properties, not allowing a more detailed analysis at a molecular level. The low solubility of $[NH_4][SCN]$ in $[C_2MIM][SCN]$ (between 0.1729 and 0.2594 in molar fraction) [38] in comparison to $[C_2MIM][C_2SO_4]$ (0.6479 in molar fraction) [37] can be a consequence of the lower ionicity of the former system since a lower ionicity indicates.

2.3.2 Thermophysical and thermodynamic properties for $[C_2MIM][SCN]$ + $[C_2MIM][DCA]$

2.3.2.1 Density and viscosity measurements

The measured density and viscosity data for the binary mixture $[C_2MIM][SCN]$ + $[C_2MIM][DCA]$ as a function $[C_2MIM][DCA]$ molar fraction at different temperatures (298.15 to 353.15 K) are given in Figure 2.13 and Figure 2.14, respectively. Figure 2.15 and 2.16 illustrate the temperature dependence of the density and viscosity, respectively, for various mixtures and compares it with the neat ILs. The experimental density and viscosity data together with the excess molar volumes and viscosity deviations at 298.15 to 353.15 K obtained in this work are listed in Table 2.5.

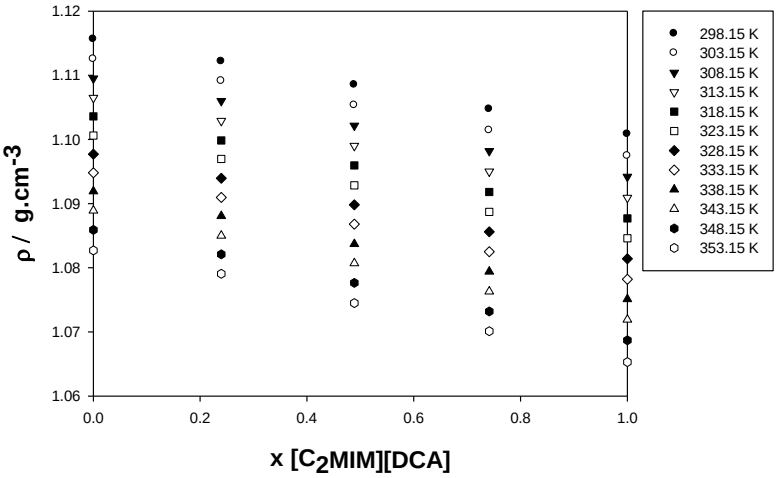

Figure 2.13 Density of the binary system [C_2MIM][SCN]+[C_2MIM][DCA]as a function of [C_2MIM][DCA] concentration .

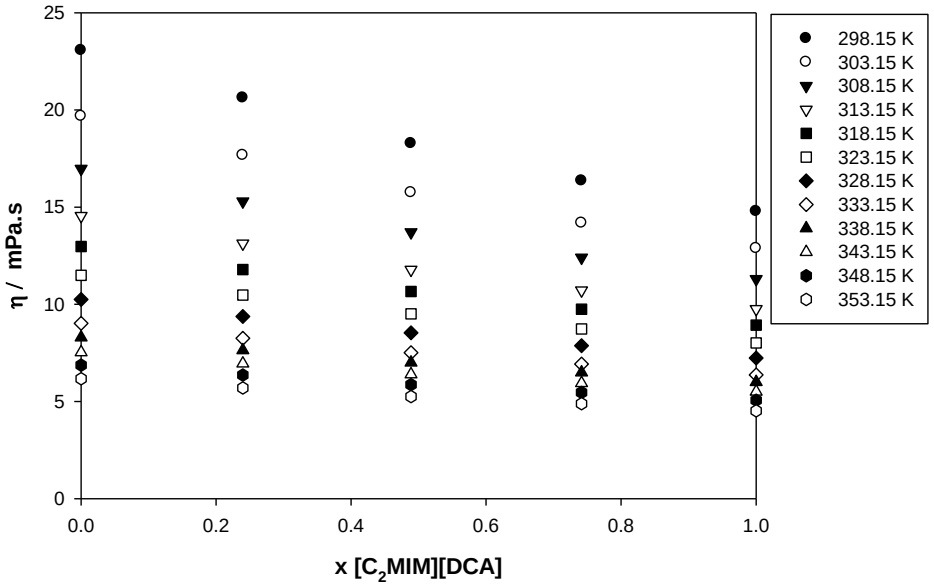

Figure 2.14 Dynamic viscosity of the binary system [C_2MIM][SCN]+[C_2MIM][DCA] as a function of [C_2MIM][DCA] concentration.

As for the [C_2MIM][SCN] + [NH_4][SCN] system, the temperature behaviour of the density, viscosity and conductivity data was described by fitting Equations 2.2 and 2.3,

respectively. The corresponding parameters are shown in Table A.3 in Appendix A.

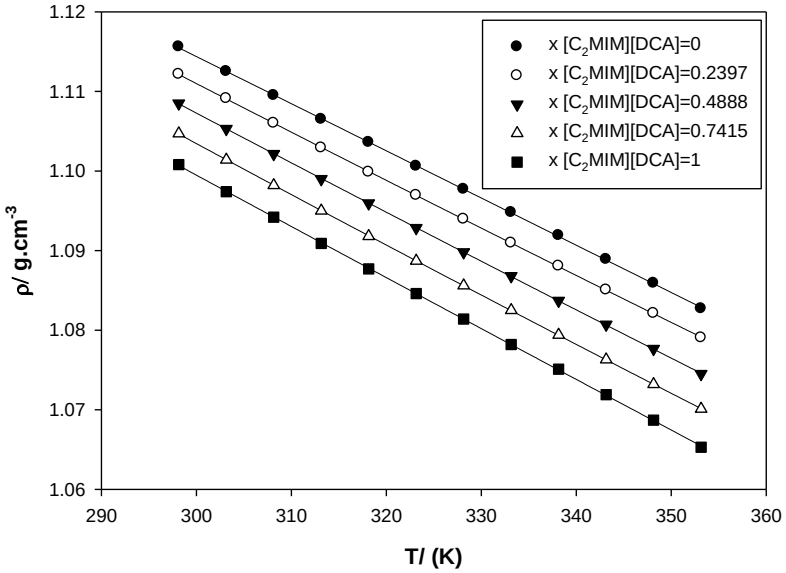

Figure 2.15 Density as a function of temperature for the $[C_2MIM][SCN]+[C_2MIM][DCA]$ binary mixtures.

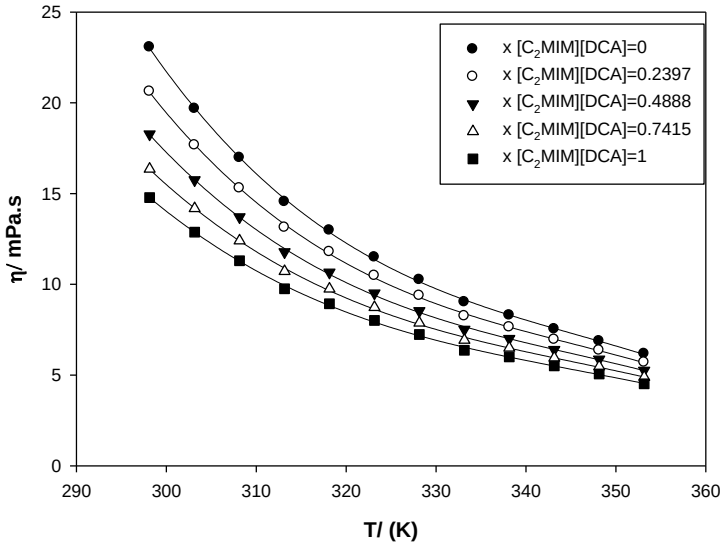

Figure 2.16 Viscosity as a function of temperature for the $[C_2MIM][SCN]+[C_2MIM][DCA]$ binary mixtures.

The excess molar volumes (V^E) resulting from the IL mixtures were calculated by Equation 2.7:

$$V^E = \frac{x_1M_1+x_2M_2}{\rho_M} - \frac{x_1M_1}{\rho_1} - \frac{x_2M_2}{\rho_2} \quad \textbf{(2.7)}$$

where ρ and x are densities and molar fractions from, respectively, the two pure IL, identified with subscript numbers and subscript M refers to the IL mixture. The excess molar volumes at 298.15K are depicted in Figure 2.17.

The viscosity deviations ($\Delta\eta$) resulting from the IL mixtures were calculated by Equation 2.8:

$$\Delta \ln(\eta) = \ln(\eta_M) - [x_1 \ln(\eta_1) + (1 - x_1) \ln(\eta_2)] \quad \textbf{(2.8)}$$

where η and x are respectively, viscosities and molar fractions from the two pure ILs identified with subscript numbers. Subscript M refers to the IL mixture. The viscosity deviations calculated at 298.15 K are represented in Figure 2.18.

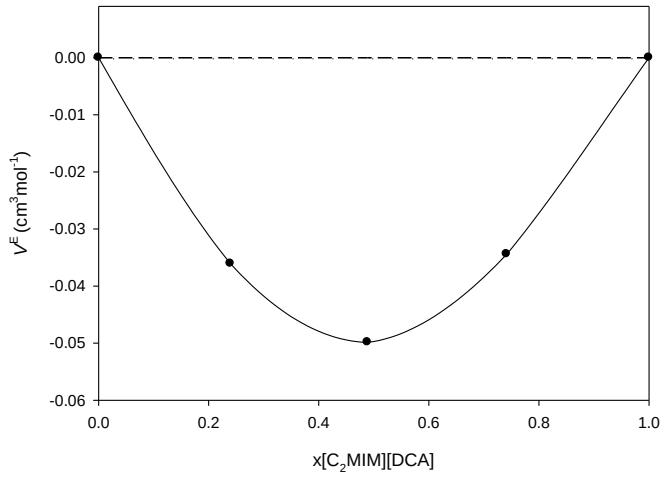

Figure 2.17 Excess molar volume of the [C_2MIM][SCN]+[C_2MIM][DCA] binary mixture at 298.15 K. The lines are guide to the eye only.

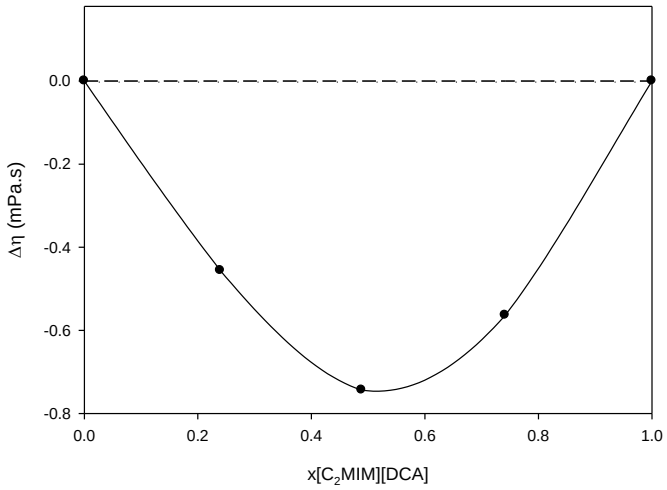

Figure 2.18 Viscosity deviations of the [C_2MIM][SCN]+[C_2MIM][DCA] binary mixture at 298.15 K. The lines are guide to the eye only.

Table 2.5 Density, ρ, viscosity, η, ionic conductivity, excess molar volumes, V^E and viscosity deviations, $\Delta\eta$ for the binary mixtures [C_2MIM][SCN](1) + [C_2MIM][DCA](2) at several temperatures

x_2	ρ (g.cm^{-3})	η (mPa.s)	V^E (cm^3.mol^{-1})	$\Delta\eta$ (mPa.s)
		298.15 K		
0	1.1156	23.0620	0	0
0.2397	1.1122	20.6200	-0.03608	-0.4560
0.4888	1.1085	18.2690	-0.04987	-0.7438
0.7415	1.1047	16.3560	-0.03443	-0.5636
1	1.1008	14.7780	0	0
		303.15 K		
0	1.1125	19.6770	0	0
0.2397	1.1091	17.6620	-0.05383	-0.3843
0.4888	1.1053	15.7445	-0.05757	-0.6077
0.7415	1.1014	14.1800	-0.03849	-0.4534
1	1.0974	12.8750	0	0
		308.15 K		
0	1.1095	16.9720	0	0
0.2397	1.1060	15.2960	-0.04724	-0.3167
0.4888	1.1022	13.7045	-0.05100	-0.4960
0.7415	1.0982	12.4030	-0.03162	-0.3648
1	1.0942	11.3020	0	0
		313.15 K		
0	1.1065	14.5430	0	0
0.2397	1.1029	13.1245	-0.04415	-0.2715
0.4888	1.0990	11.7825	-0.05163	-0.4219
0.7415	1.0950	10.7180	-0.03572	-0.2775
1	1.0909	9.7586	0	0

		318.15 K		
0	1.1036	12.9760	0	0
0.2397	1.0999	11.7885	-0.03395	-0.2172
0.4888	1.0960	10.6565	-0.05226	-0.3411
0.7415	1.0918	9.7503	-0.02516	-0.2247
1	1.0877	8.9286	0	0
		323.15 K		
0	1.1006	11.4880	0	0
0.2397	1.0970	10.4730	-0.05199	-0.1812
0.4888	1.0929	9.5083	-0.04544	-0.2796
0.7415	1.0887	8.7300	-0.02171	-0.1790
1	1.0846	8.0098	0	0
		328.15 K		
0	1.0977	10.2460	0	0
0.2397	1.0940	9.374	-0.04888	-0.1507
0.4888	1.0898	8.536	-0.04606	-0.2381
0.7415	1.0856	7.871	-0.02583	-0.1428
1	1.0814	7.235	0	0
		333.15 K		
0	1.0948	9.020	0	0
0.2397	1.0910	8.250	-0.04574	-0.1335
0.4888	1.0868	7.515	-0.05402	-0.2087
0.7415	1.0825	6.923	-0.02999	-0.1295
1	1.0782	6.367	0	0
		338.15 K		
0	1.0919	8.297	0	0
0.2397	1.0881	7.640	-0.05335	-0.1075
0.4888	1.0837	7.006	-0.03984	-0.1696
0.7415	1.0794	6.493	-0.02285	-0.1024
1	1.0751	6.002	0	0
		343.15 K		
0	1.0889	7.532	0	0
0.2397	1.0851	6.953	-0.06106	-0.0942
0.4888	1.0807	6.396	-0.05516	-0.1462
0.7415	1.0763	5.942	-0.03074	-0.0892
1	1.0719	5.508	0	0
		348.15 K		
0	1.0859	6.870	0	0
0.2397	1.0821	6.358	-0.07616	-0.0787
0.4888	1.07765	5.867	-0.06321	-0.1208
0.7415	1.0732	5.465	-0.03874	-0.0661
1	1.0687	5.064	0	0
		353.15 K		
0	1.0827	6.169	0	0
0.2397	1.0791	5.700	-0.10618	-0.0733
0.4888	1.0745	5.251	-0.08638	-0.1118
0.7415	1.0701	4.888	-0.07744	-0.0581
1	1.0653	4.520	0	0

It can be seen that the density values of the mixture are in between those of the pure ILs, as expected. Regarding the volume changes of a mixture, those can be the result of chemical, physical and structural modifications. Physical contributions cause positive V^E values resulting from non-specific interactions between the real species present in the mixture. The chemical interactions that include charge-transfer type forces, changes in hydrogen bonding equilibrium or electrostatic interactions, as well as the structural contributions that arise from geometrical fitting, contribute to negative V^E values, as is the case of the $[C_2MIM][SCN]$ + $[C_2MIM][DCA]$ mixtures studied in this work.

Taking into account Table 2.5, the viscosity trend is similar to that of the density. The viscosity values of the IL mixtures are in between those of the two pure ILs. Concerning the viscosity deviations, charge transfer and hydrogen bonding interactions lead to positive $\Delta\ln(\eta)$ values, whereas negative values are usually obtained for systems where molecular size and shapes of the components and dispersion and dipolar interactions are considered. In this case, deviations in viscosity cannot be strictly justified by the size effects, since the ions present are very similar in size and shape. The negative viscosity values mean that the favourable interactions that occur between the ions of the mixture in the whole composition range, as a result of $V^E < 0$, occur through weak forces such as dispersion forces or dipolar interactions.

2.3.2.2 Ionic Conductivity

Figure 2.19 shows a comparison of the behaviour of the ionic conductivity between the neat ILs and the binary mixtures prepared in this work. This data is listed in Table 2.6.

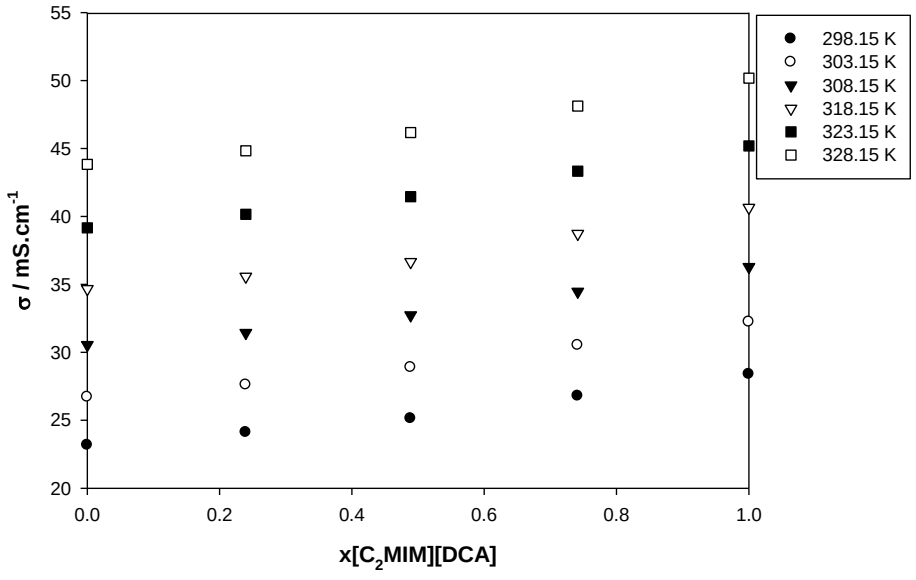

Figure 2.19 Ionic conductivity as a function of $[C_2MIM][DCA]$ molar fraction for the binary system $[C_2MIM][SCN]$+ $[C_2MIM][DCA]$.

Table 2.6 Ionic conductivity, σ, for the binary system $[C_2MIM][SCN](1) + [C_2MIM][DCA]$ (2) at several temperatures.

	σ/ (mS.cm^{-1})					
x_2	**298.15 K**	**303.15 K**	**308.15 K**	**313.15 K**	**318.15 K**	**323.15 K**
0	23.17	26.70	30.55	34.66	39.15	43.83
0.2397	24.10	27.60	31.43	35.57	40.15	44.83
0.4888	25.12	28.88	32.72	36.65	41.45	46.17
0.7415	26.78	30.51	34.46	38.72	43.33	48.12
1	28.38	32.23	36.28	40.64	45.18	50.17

2.3.2.3 Walden Plot

Figure 2.20 shows the Walden plot for the binary system $[C_2MIM][SCN]$ + $[C_2MIM][DCA]$ and Figure 2.21 shows the deviations from the "ideal" behaviour which allow the evaluation of the system's ionicity.

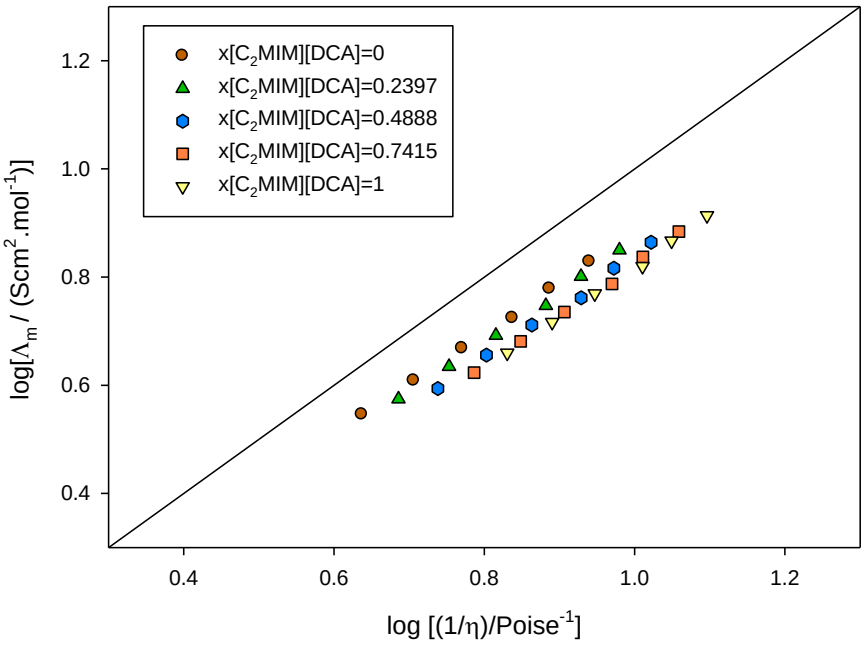

Figure 2.20 Walden plot for the binary system $[C_2MIM][SCN]+[C_2MIM][DCA]$.

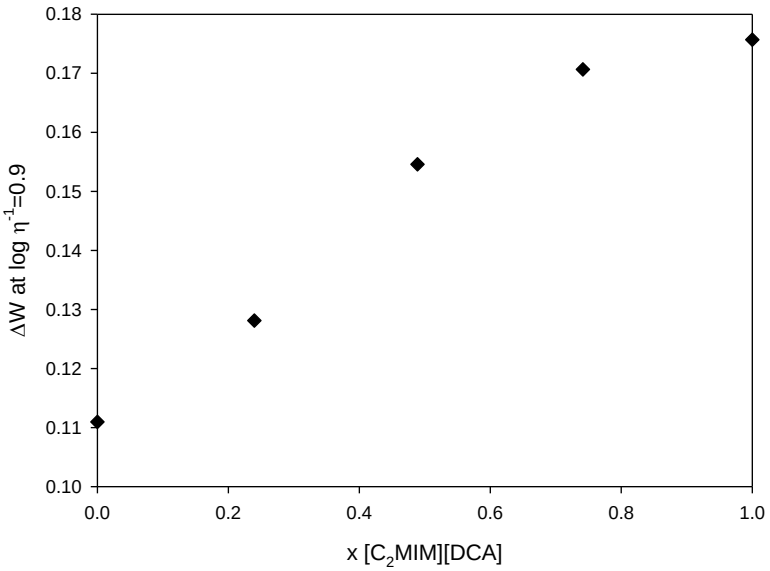

Figure 2.21 Deviations from the "ideal" Walden behaviour as a function of $[C_2MIM][DCA]$ molar fraction

It can be observed that the ionic liquid mixtures present an ionicity that falls between the pure ILs, where pure $[C_2MIM][SCN]$ shows a greater ionicity than $[C_2MIM][DCA]$. Therefore, it could be interpreted that adding the thiocyanate based IL to the dicyanamide based IL improves the ionicity of the latter. This mixture was chosen due to the low viscosity and density and the high conductivity of the ILs involved compared to other ILs.

2.3.3 Thermophysical and thermodynamic properties for $[C_2MIM][SCN] + [C_2MIM][C_2SO_4]$

2.3.3.1. Density and viscosity measurements

The measured density and viscosity data for the binary mixture $[C_2MIM][SCN] + [C_2MIM][C_2SO_4]$ as a function of $[C_2MIM][C_2SO_4]$ molar fraction at different temperatures (from 298.15 to 353.15 K) are shown in Figure 2.22 and Figure 2.23, respectively. Figure 2.24 and Figure 2.25 illustrate the temperature dependence of the density and viscosity, respectively, for $[C_2MIM][SCN] + [C_2MIM][C_2SO_4]$ binary mixtures and compares it with the neat ILs. Table 2.7 shows the density and viscosity data, as well as the excess molar volumes and viscosity deviations at several temperatures.

As for the $[C_2MIM][SCN]$ + $[NH_4][SCN]$ system, the temperature behaviour of the density, viscosity and conductivity data was described by fitting Equations 2.2 and 2.3, respectively. The corresponding parameters are shown in Table A.4 in Appendix A.

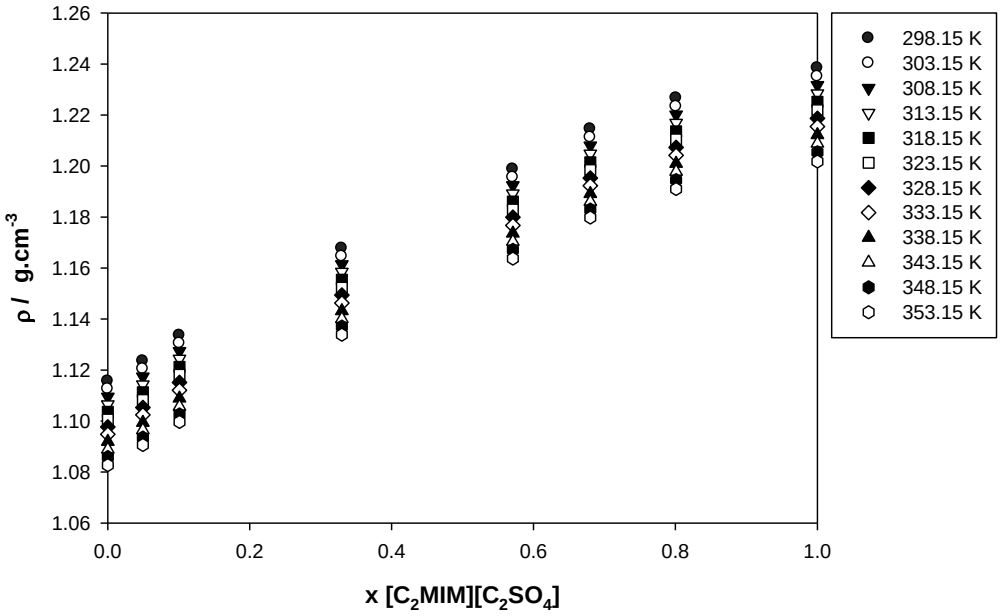

Figure 2.22 Density of the binary mixture $[C_2MIM][[SCN]+[C_2MIM][C_2SO_4]$ as a function of $[C_2MIM][C_2SO_4]$ molar fraction.

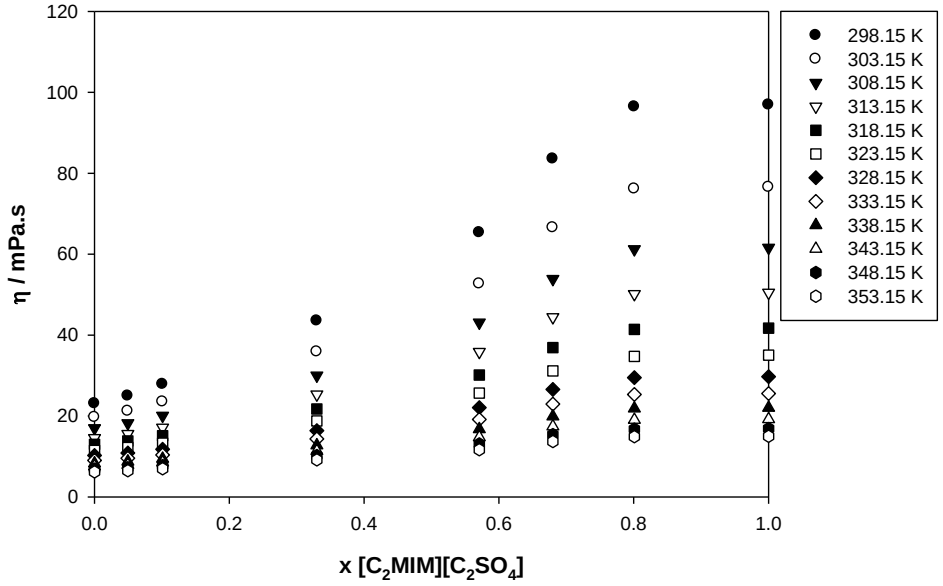

Figure 2.23 Viscosity of the binary mixture $[C_2MIM][[SCN]+[C_2MIM][C_2SO_4]$ as a function of $[C_2MIM][C_2SO_4]$ molar fraction

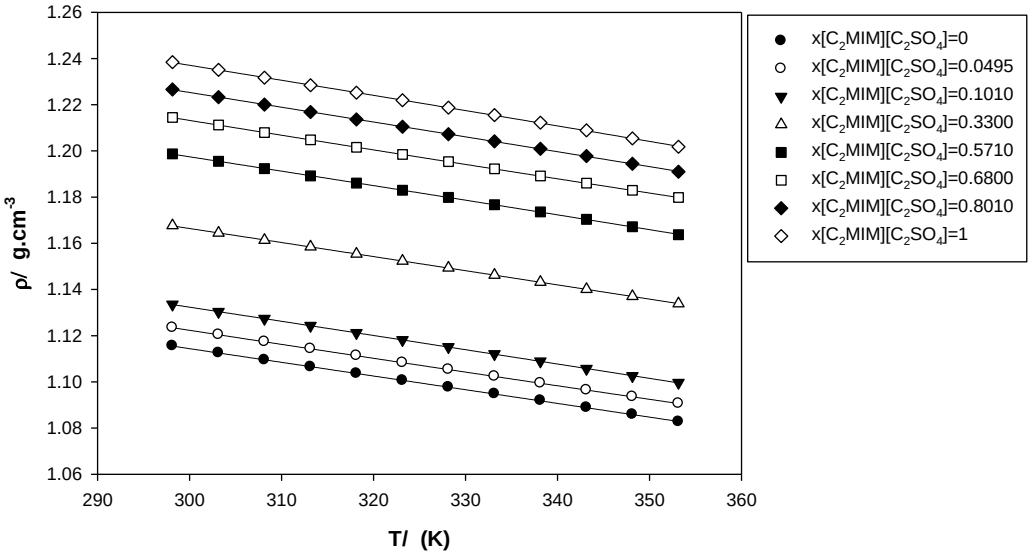

Figure 2.24 Density as a function of temperature for the $[C_2MIM][[SCN]+[C_2MIM][C_2SO_4]$binary mixtures.

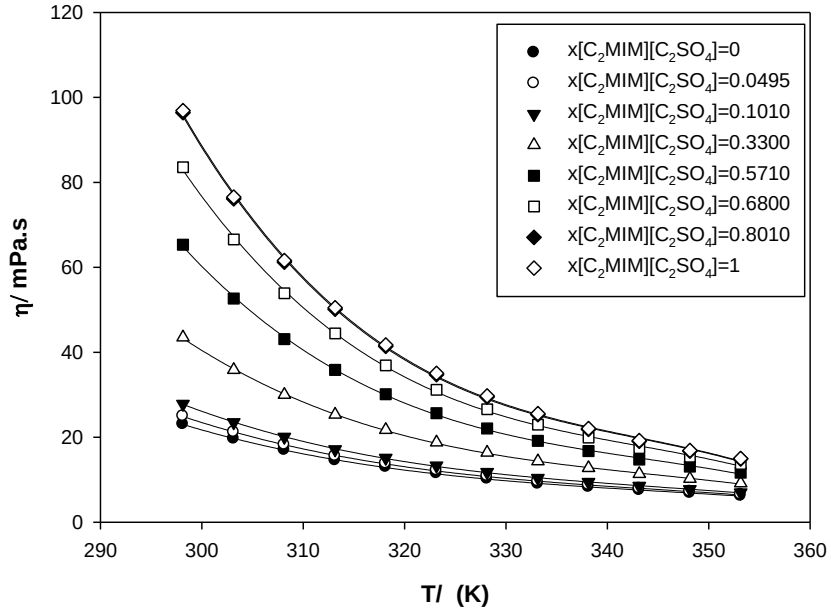

Figure 2.25 Viscosity of the binary mixture $[C_2MIM][[SCN]+[C_2MIM][C_2SO_4]$ as a function of temperature.

Figure 2.26 and 2.27 show the excess molar volumes and viscosity deviations, respectively, of the $[C_2MIM][[SCN]+[C_2MIM][C_2SO_4]$ system at 298.15 K.

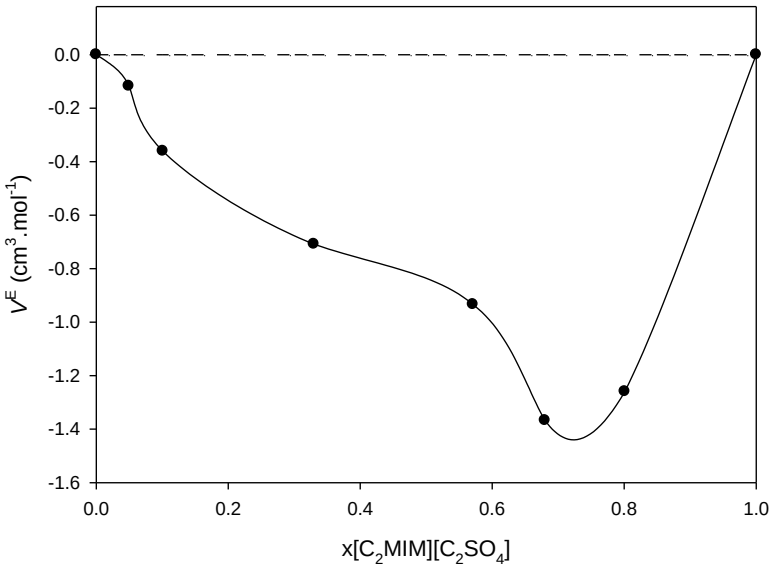

Figure 2.26 Excess molar volume of the $[C_2MIM][SCN]+[C_2MIM][C_2SO_4]$ at 298.15 K. The lines are guide to the eye only

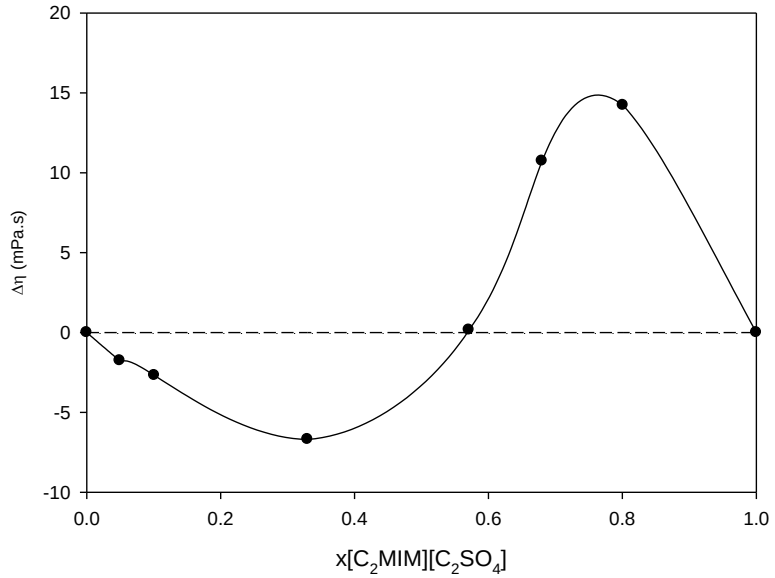

Figure 2.27 Viscosity deviations of the ionic liquid mixture at 298.15 K. The lines are guide to the eye only

Table 2.7 Density, ρ, viscosity, η, ionic conductivity, excess molar volumes, V^E and viscosity deviations, $\Delta\eta$ for the binary mixtures $[C_2MIM][SCN]$ (1) + $[C_2MIM][C_2SO_4]$ (2) at several temperatures

x_2	ρ (g.cm^{-3})	η (mPa.s)	V^E (cm^3.mol^{-1})	$\Delta\eta$ (mPa.s)
		298.15 K		
0	1.1156	23.0620	0	0
0.0495	1.1235	24.9540	-0.0480	-1.7614
0.1010	1.1335	27.8305	-0.3702	-2.6860
0.3300	1.1677	43.5020	-0.7155	-3.9163
0.5710	1.1987	65.3315	-0.9096	0.1534
0.6800	1.2145	83.5445	-1.3852	10.7312
0.8010	1.2266	96.3990	-1.2616	14.2176
1	1.2384	96.8690	0	0
		303.15 K		
0	1.1125	19.6770	0	0
0.0495	1.1204	21.1960	-0.0500	-1.2945
0.1010	1.1304	23.4970	-0.3690	-1.9206
0.3300	1.1645	35.8440	-0.7166	-2.5895
0.5710	1.1955	52.6510	-0.9187	0.5408
0.6800	1.2112	66.5260	-1.3998	8.5302
0.8010	1.2233	76.1280	-1.2637	10.9238
1	1.2351	76.5150	0	0
		308.15 K		
0	1.1095	16.9720	0	0
0.0495	1.1174	18.2040	-0.0478	-1.0416
0.1010	1.1274	20.0725	-0.3846	-1.4070
0.3300	1.1614	29.9840	-0.7278	-1.7156
0.5710	1.1924	43.1135	-0.9381	0.6751
0.6800	1.2080	53.8705	-1.4059	6.7923
0.8010	1.2201	61.2035	-1.2831	8.4837
1	1.2317	61.6010	0	0
		313.15 K		
0	1.1065	14.5430	0	0
0.0495	1.1143	15.5670	-0.0460	-0.8178
0.1010	1.1244	17.1270	-0.3850	-1.0476
0.3300	1.1585	25.3030	-0.7624	-1.1055
0.5710	1.1892	35.8590	-0.9488	0.7986
0.6800	1.2048	44.4085	-1.4163	5.5939
0.8010	1.2169	50.1280	-1.2977	6.7842
1	1.2284	50.4990	0	0
		318.15 K		
0	1.1036	12.9760	0	0
0.0495	1.1113	13.8260	-0.0333	-0.6280
0.1010	1.1212	15.1225	-0.3572	-0.7569
0.3300	1.1554	21.7260	-0.7543	-0.7365
0.5710	1.1861	30.1265	-0.9520	0.7467
0.6800	1.2015	36.9145	-1.4116	4.5290
0.8010	1.2136	41.4195	-1.2970	5.4172
1	1.2252	41.7230	0	0
		323.15 K		
0	1.1006	11.4880	0	0
0.0495	1.1083	12.2030	-0.0368	-0.5001
0.1010	1.1182	13.3010	-0.3574	-0.5643
0.3300	1.1524	18.7790	-0.7750	-0.4765

0.5710	1.1830	25.6520	-0.9702	0.7326
0.6800	1.1985	31.1395	-1.4370	3.7562
0.8010	1.2105	34.7435	-1.3117	4.4016
1	1.2219	35.0260	0	0
		328.15 K		
0	1.0977	10.2460	0	0
0.0495	1.1053	10.8560	-0.0282	-0.3545
0.1010	1.1151	11.7840	-0.3434	-0.4299
0.3300	1.1494	16.3790	-0.7813	-0.2967
0.5710	1.1799	22.0530	-0.9661	0.6889
0.6800	1.1953	26.5585	-1.4473	3.1539
0.8010	1.2073	29.4835	-1.3111	3.6308
1	1.2187	29.7300	0	0
		333.15 K		
0	1.0948	9.0199	0	0
0.0495	1.1024	9.5558	-0.0209	-0.2824
0.1010	1.1121	10.3740	-0.3292	-0.3155
0.3300	1.1463	14.3520	-0.7731	-0.1232
0.5710	1.1767	19.1405	-0.9620	0.6875
0.6800	1.1923	22.9335	-1.4578	2.7480
0.8010	1.2042	25.3285	-1.3258	3.0672
1	1.2155	25.5510	0	0
		338.15 K		
0	1.0919	8.2973	0	0
0.0495	1.0994	8.7492	-0.0161	-0.2282
0.1010	1.1089	9.4458	-0.3021	-0.2392
0.3300	1.1432	12.7590	-0.7701	-0.0721
0.5710	1.1736	16.7365	-0.9744	0.5996
0.6800	1.1891	19.8925	-1.4792	2.3134
0.8010	1.2010	21.8500	-1.3381	2.5480
1	1.2122	22.0360	0	0
		343.15 K		
0	1.0889	7.5322	0	0
0.0495	1.0965	7.9189	-0.0272	-0.1921
0.1010	1.1057	8.5285	-0.2804	-0.1848
0.3300	1.1401	11.3750	-0.7766	-0.0162
0.5710	1.1704	14.7455	-0.9780	0.5405
0.6800	1.1860	17.4260	-1.5055	1.9920
0.8010	1.1978	19.0605	-1.3533	2.1616
1	1.2089	19.2260	0	0
		348.15 K		
0	1.0859	6.8699	0	0
0.0495	1.0935	7.2061	-0.0413	-0.1600
0.1010	1.1026	7.7415	-0.2761	-0.1409
0.3300	1.1370	10.2060	-0.8013	0.0281
0.5710	1.1671	13.0775	-0.9925	0.4876
0.6800	1.1829	15.3835	-1.5541	1.7437
0.8010	1.1945	16.7535	-1.3791	1.8543
1	1.2054	16.8940	0	0
		353.15 K		
0	1.0827	6.1691	0	0

0.0495	1.0906	6.4757	-0.0863	-0.1305
0.1010	1.0997	6.9649	-0.3213	-0.0960
0.3300	1.1339	9.1617	-0.8361	0.0787
0.5710	1.1638	11.6815	-1.0060	0.4738
0.6800	1.1798	13.7070	-1.6236	1.5766
0.8010	1.1910	14.8720	-1.4004	1.6302
1	1.2018	14.9990	0	0

Identically to the system [C_2MIM][SCN]+[C_2MIM][DCA], it can be seen that the density values of the mixture are in between those of the pure ILs. Regarding the volume changes of the mixture, negative values of this property were obtained for the entire composition range indicating that favourable interactions take place when these two ILs are mixed.

Taking into account Table 2.7, the viscosity trend is similar to that of the density. The viscosity values of the IL mixtures are in between those of the two pure ILs. However, the viscosity changes are smaller in mixtures that are progressively richer in [C_2MIM][C_2SO_4] than when the mixture is gradually richer in [C_2MIM][SCN]. This is explained by the large difference in viscosity between the pure thiocyanate-based IL and the ethyl sulfate-based IL, in comparison to the viscosities of the pure [C_2MIM][SCN] and [C_2MIM][DCA] used in the previous study. Concerning the viscosity deviations, Figure 2.27 shows negative values for mixtures rich in [C_2MIM][SCN] up to an approximately equimolar mixture, where $\Delta\ln(\eta)$ is approximately zero, and then positive deviations were obtained for mixtures rich in [C_2MIM][C_2SO_4].

2.3.3.2 Ionic Conductivity

Figure 2.28 shows the behaviour of the ionic conductivity of the IL mixtures and Table 2.8 lists the data at various temperatures.

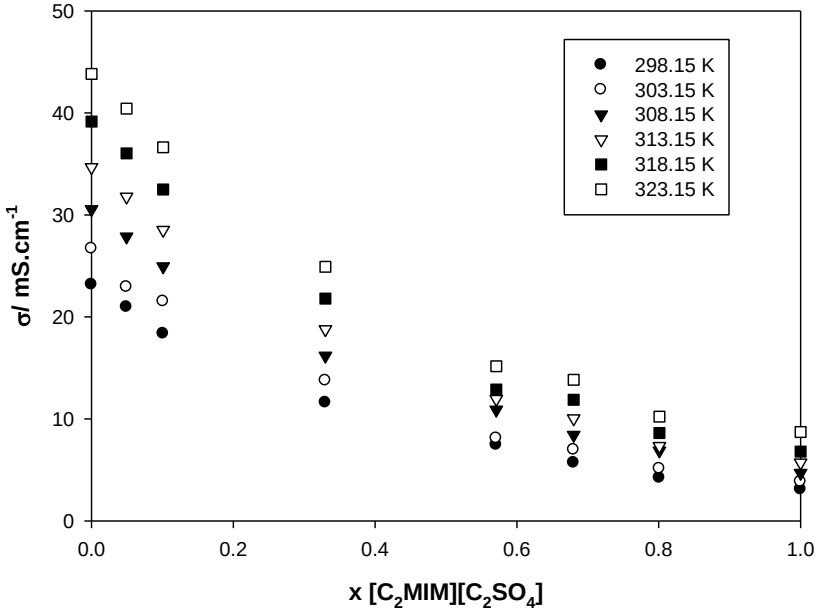

Figure 2.28 Ionic conductivity of the binary system $[C_2MIM][SCN]$+ $[C_2MIM][C_2SO_4]$as a function of $[C_2MIM][C_2SO_4]$.

Table 2.8 Ionic conductivity, σ, for the binary system $[C_2MIM][SCN]$ (1) + $[C_2MIM][C_2SO_4]$ (2) at several temperatures.

	σ/ (mS.cm^{-1})					
x_2	**298.15 K**	**303.15 K**	**308.15 K**	**313.15 K**	**318.15 K**	**323.15 K**
0	23.17	26.70	30.55	34.66	39.15	43.83
0.0495	20.97	22.92	27.87	31.78	36.04	40.42
0.1010	18.36	21.52	24.95	28.52	32.49	36.63
0.3300	11.60	13.75	16.18	18.78	21.79	24.92
0.5710	7.45	8.09	10.89	11.94	12.88	15.16
0.6800	5.69	6.96	8.42	10.04	11.88	13.83
0.8010	4.21	5.12	6.88	7.33	8.61	10.23
1	3.08	3.82	4.69	5.70	6.78	8.71

2.3.3.3 Walden Plot

Figure 2.29 shows the Walden plot for the binary system [C_2MIM][SCN] + [C_2MIM][C_2SO_4] and Figure 2.30 shows the deviations from the "ideal" behaviour which allow the evaluation of the system's ionicity.

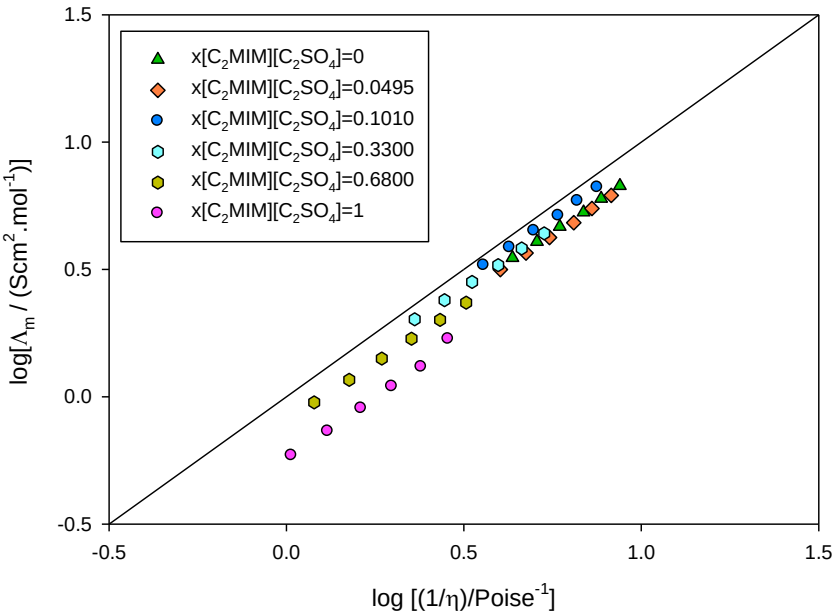

Figure 2.29 Walden plot for the binary system [C_2MIM][SCN]+[C_2MIM][C_2SO_4].

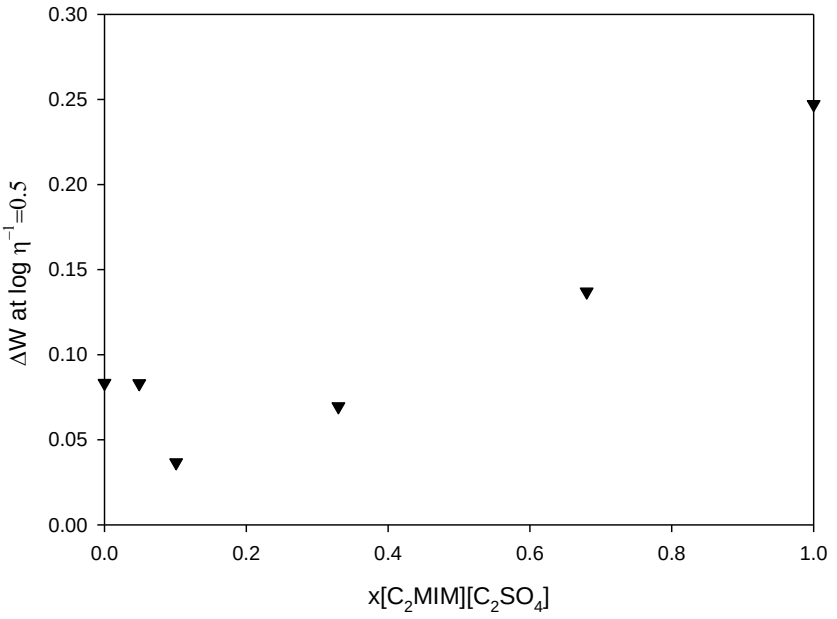

Figure 2.30 Deviations from the "ideal" Walden behaviour as a function of [C_2MIM][C_2SO_4] molar fraction.

From the analysis of Figure 2.30 it can be observed that unlike the previous system where [C_2MIM][SCN] was mixed with [C_2MIM][DCA], the ionicity of the ionic liquid mixtures do not all fall between the ionicity of the pure ILs. The deviation from the "ideal" behaviour decreases as small amounts of [C_2MIM][C_2SO_4] are added to [C_2MIM][SCN] and apparently reaches the lowest deviation when the mixture is composed of approximately 10% in molar fraction of [C_2MIM][C_2SO_4]. From this point onwards the ionicity decreases as the ethyl sulfate-based IL is added to the system, until the highest deviation of this system is reached, which corresponds to the pure [C_2MIM][C_2SO_4]. Therefore, it can be interpreted that, for this particular system, a mixture containing a well-defined molar composition of 90% [C_2MIM][SCN] and 10% [C_2MIM][C_2SO_4] presents maximum ionicity, that is the maximum mobility of the ions.

2.4 Solvent selection for the azeotrope separation

Figure 2.31 shows a comparison between the ionicity of the three systems studied in this work: [C_2MIM][SCN]+[NH_4][SCN], [C_2MIM][SCN]+[C_2MIM][DCA] and [C_2MIM][SCN]+[C_2MIM][C_2SO_4], in terms of deviations from the "ideal" Walden behaviour. The deviations are plotted as a function of the molar composition of the component that was added to [C_2MIM][SCN] and were all determined at a constant fluidity of $\log(\eta^{-1}) = 0.5$. This fluidity was chosen to avoid, as much as possible, the extrapolation of the experimental points in order to measure the difference between these and the "ideal" line. Therefore, by analysing each Walden plot separately, it was possible to see that only one of the systems' observed points had to be, unavoidably, extrapolated, so that a proper comparison could be made.

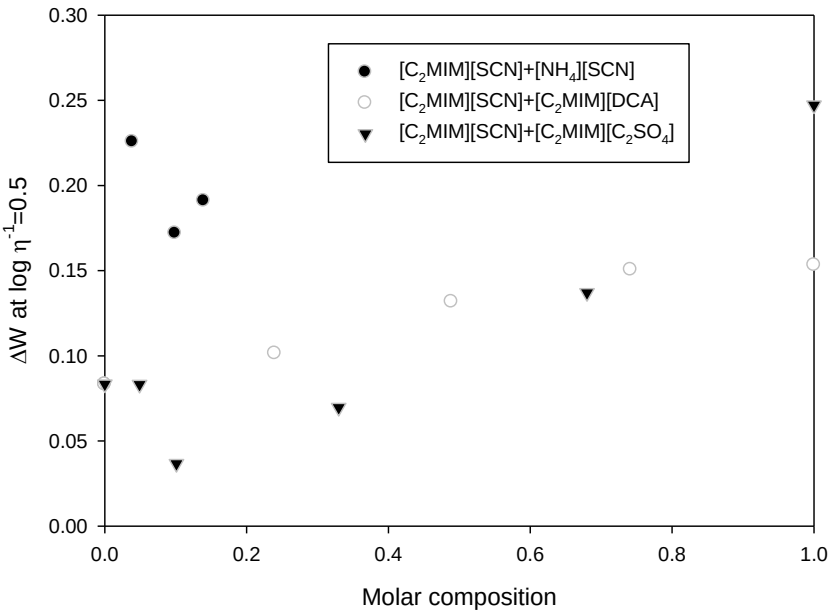

Figure 2.31 Deviations from the "ideal" Walden behaviour as a function of the molar fraction of component added to [C_2MIM][SCN].

It can be observed that, at a chosen constant fluidity, the [C_2MIM][SCN]+[C_2MIM][C_2SO_4] binary mixture presents a lower deviation from the "ideal" Walden behaviour than the other systems studied, for most of the composition range. Out of the three systems, the mixture [C_2MIM][SCN]+[C_2MIM][DCA] presents the lowest variation in ionicity throughout the whole composition range, indicating that mixing the dicyanamide based IL with the thiocyanate based IL does not lead to a significant modification in ionicity compared to the other systems. This result was expected due to the very similar chemical nature of the two ILs.

Therefore, the solvent chosen to proceed to the liquid-liquid equilibria study was the mixture [C_2MIM][SCN]$_{0.9}$[C_2SO_4]$_{0.1}$ as it has the lowest deviation from the "ideal" Walden behaviour of the systems studied, and thus, presents the highest ionicity.

2.5 Conclusions

The objective of this chapter was to evaluate the ionicity of three systems, all based on [C_2MIM][SCN], one in which an inorganic salt was added to an ionic liquid and the remaining consisting of a mixture of two ILs. After performing the thermodynamic study, indispensable for the determination of the ionicity of the systems, it was possible to conclude that solubilizing ammonium thiocyanante in pure [C_2MIM][SCN] does not yield a system with increased ionicity, consequently not forming a high ionicity ionic liquid. The fact that the addition of the salt increased the viscosity of the pure [C_2MIM][SCN] and, consequently, decreased the ionic conductivity is also behind the explanation of the mixtures presenting a lower ionicity than the pure IL. Another possible explanation could be based on the fact that the IS and the IL have thiocyanate as the common anion, unlike studies where [NH_4][SCN] was solubilized in ILs without a common anion, such as [C_2MIM][C_2SO_3] and [C_2MIM][C_2SO_4], where the increase in ionicity was justified by the hydrogen bonds established between the NH_4^+ cation and the anion of the IL, [C_2SO_3] or [C_2SO_4] leaving the SCN^- anion "free". This suggests that the existence of a common anion may lead to lack of "competitiveness" between the ions involved in the system.

The mixtures of the ILs led to very different behaviours than the dissolution of the inorganic salt in the IL. The IL+IS system presents a lower ionicity than any of the two studied ionic liquid mixtures, due to the greater Walden deviation. Moreover, the mixtures of ILs present a smoother behaviour in ionicity than the IL+IS system, where the latter shows a more abrupt variation.

It can also be concluded that the mixture [C_2MIM][SCN]+[C_2MIM][DCA] shows a quasi-ideal behaviour, justified by the very small excess volumes and viscosity deviations. However, these mixtures showed negative V^E values, unlike other binary mixtures where a common anion or a common cation led to positive values of excess molar volumes[47]. In order to provide a more detailed explanation of these results, different studies need to be conducted, such as NMR, Raman spectroscopy and ATR-FTIR which can describe the behaviour on a molecular level, quantitatively.

To sum up, the solvent chosen to apply as an extraction agent in the separation of the azeotropic mixture heptane + ethanol was the ionic liquid mixture [C_2MIM][SCN]$_{0.9}$[C_2SO_4]$_{0.1}$, which

revealed the highest ionicity of the systems studied. Therefore, this highly ionic ionic liquid was used as a solvent in order to establish a possible correlation between the ionicity and the extraction efficiency in the breaking of the azeotrope, the main objective of this dissertation.

3. Liquid-Liquid Equilibria

3.1 Introduction

Liquid-liquid extraction is a method to separate compounds based on the immiscibility between the involved liquids. If a certain feed phase contains two components, *i* (solute) and j (inert), in which *i* is to be removed, the addition of a second phase, *s*, (solvent) must be immiscible or at least partially miscible with the feed phase. Ternary liquid mixtures can be classified in many forms based on their miscibility gaps, according to the classification proposed by Treybal and mentioned by Olaya et al. [48] Ternary mixtures that present closed miscibility gaps, whose binodal curve forms an island are classified as Type 0 and are commonly found in the systems formed by weak acids and bases that reversibly produce a soluble salt, which presents a limited miscibility. In Type I LLE, component, j and s are immiscible or partly miscible and *i* is totally soluble in *j* or *s*. Type II classifies a system in which both pairs, *i* and *j*, or *i* and *s* are partially miscible. As is the case in this dissertation, component *i* dissolves in both phases, so it is transferred from the feed to the solvent phase, consequently purifying component *j*. The solute can then be separated from the solvent by a technique such as distillation and the latter is regenerated and can be reused so long as there is no raffinate in the extract. The ease of this final separation is one of the important factors to be considered when selecting the extraction solvent. Other factors include chemical reactivity, viscosity, vapour pressure, flammability, toxicity, selectivity and distribution coefficient (described in more detail in Chapter 3.1.2), etc. Thus, ILs possess almost all of the requirements for a suitable solvent.

In this chapter, the separation of the binary mixture of heptane and ethanol was studied through the use highly ionic ILs as solvents. As proposed in the last chapter, one pure IL, $[C_2MIM][SCN]$, and one binary mixture of ILs composed of $[C_2MIM][SCN]$ and $[C_2MIM][C_2SO_4]$, at a molar fraction composition of 0.9 and 0.1, are proposed as highly ionic ILs. With the intuit of evaluating if the ionicity of an IL is related to its extractive and selective capacity of ethanol from the heptane + ethanol mixture, ternary liquid-liquid equilibria phase diagrams using pure $[C_2MIM][SCN]$ and the IL mixture $[C_2MIM][SCN]_{0.9}[C_2SO_4]_{0.1}$ were experimentally determined and the selectivity and distribution coefficient evaluated.

3.1.1 Plotting Ternary Diagrams and Tie-Lines

To be able to implement a separation process, the accurate knowledge and control of the thermodynamic properties of the mixture, as well as phase equilibria behaviour is required. A convenient way of understanding the liquid-liquid equilibria of a ternary system is by plotting it on an equilateral triangle diagram, which has three axes, usually representing mole or mass fractions. Each triangle vertex denotes a pure chemical and the mass or molar fraction of each component can be read by drawing projections parallel to each base through a certain mixture

point. Figure 3.1 shows how the composition of a mixture can be determined. Species A, B and C are the pure components and point M represents the composition of a ternary mixture within the immiscibility boundary. Any point outside the immiscibility zone corresponds to a single-phase mixture. By using the lines parallel to the edge opposite the corner corresponding to the pure component, the composition of the mixture can be read. Therefore, the mixture with the composition denoted by M is composed of 40% of A, 20% of B and the remaining 40% of C. This ternary mixture separates into two phases and their compositions (E and R) are given by a tie-line that passes through M. R is the raffinate and represents the liquid stream which remains after the solute (ethanol) is partially or totally removed from the azeotropic mixture through contact with the solvent. The extract, E, is the product containing the removed compound (ethanol) and the solvent (ionic liquid) [49,50].

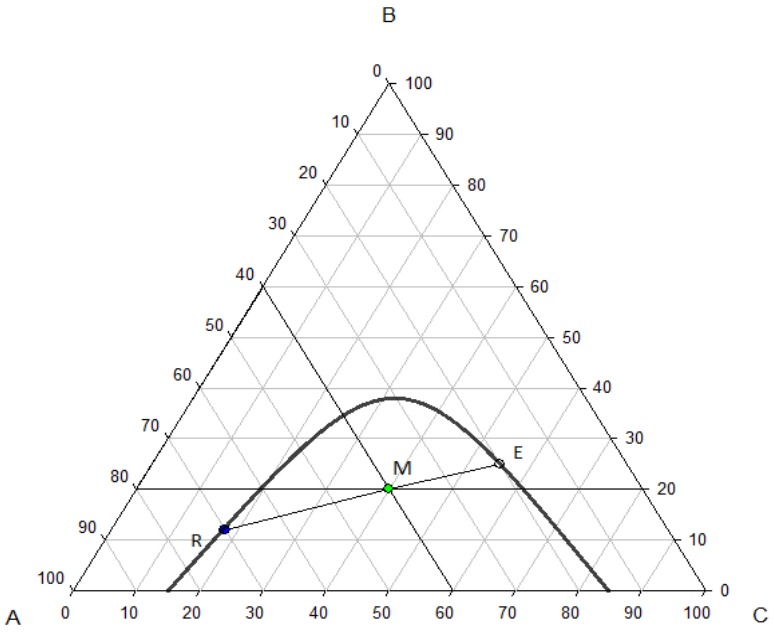

Figure 3.1 Ternary diagram of an arbitrary LLE data. The line RME represents a tie-line, M a starting point, R the raffinate and E the extract.

3.1.2 Selectivity and Distribution Coefficient

The distribution coefficient, β and the selectivity, S, there are two parameters widely used to characterize the suitability of a solvent in a liquid-liquid extraction process and are defined as follows:

$$\boldsymbol{\beta} = \frac{w_2^{IL-rich\ phase}}{w_2^{Heptane-rich\ phase}} \qquad \textbf{(3.1)}$$

$$S = \frac{w_2^{IL-rich\ phase} w_1^{Heptane-rich\ phase}}{w_2^{Heptane-rich\ phase} w_1^{IL-rich\ phase}} \qquad (3.2)$$

where w is the mass fraction and subscripts 1 and 2 correspond to the heptane and ethanol, respectively.

The distribution coefficient describes the solute-carrying capability of the solvent (pure and mixture of ILs) and it determines the amount of solvent required for the extraction process. Selectivity indicates the separation power of the ionic liquid, indicating the ease of extraction of a certain solute from an inert (heptane). The ideal extraction solvent should present high values of both β and S, since high distribution coefficients imply a lower solvent flow rate, a smaller diameter column and consequently, a lower operating cost. A great selectivity would decrease the number of equilibrium stages needed in an extraction unit and fewer amounts of inert residual would remain in the extract.

3.2 Materials and Experimental Procedure

3.2.1 Materials

Both the pure IL [C_2MIM][SCN] and the binary mixture of [C_2MIM][SCN]$_{0.9}$[C_2SO_4]$_{0.1}$ were obtained as previously referred in Chapter 2. A single batch of the mixture was prepared and dried in a round-bottom flask with a total volume of about 100ml to ensure that the solvent used throughout the whole LLE experiment had exactly the same composition and thus presented the same thermodynamic properties. The mixture was prepared with an uncertainty of $\pm 1.5.10^{-4}$in mass fraction. The components of the azeotropic mixture were heptane and ethanol. These were purchased from Carlo Erba (99% wt) and Panreac (99.5% wt), respectively, and used without any further purifications.

3.2.2 Experimental Procedure

The ternary liquid-liquid equilibrium experiments were performed at 25^{0}C in a glass cell containing a magnetic stirrer. The cell was provided with an external jacket in which water circulated at the working temperature (± 0.01K) using a Lauda E200 water thermostat and a Pt 100 probe coupled to a Keithley 199 System DMM/Scanner.

Two different experimental procedures were used to study the ternary LLE of heptane + ethanol + solvent: the first is based on the direct determination of the binodal curve, by

pinpointing the disappearance of the turbidity (cloud point) ;the second is centred on the determination of the tie-lines, by calculating the composition of each phase in equilibrium using previously established calibration curves. The binodal curve of the heptane + ethanol + solvent ternary system was determined by preparing mixtures of the solvent (ionic liquid) and inert (heptane) in the immiscible region. The mixture was placed inside of the jacketed cell and properly stirred for 30 minutes, to guarantee thermostatization as well as good mixing. Known quantities of ethanol were then carefully added and the mixture was stirred again. The procedure was repeated until the ternary mixture became totally miscible, that is, the "cloud point" of the mixture is determined (Figure 3.2).

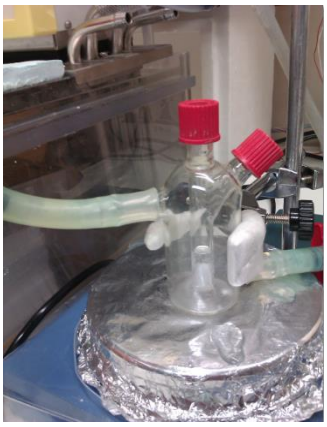

Figure 3.2 Jacketed glass cell used in this work for the determination of the LLE.

For the determination of the tie-lines (Figure 3.3), about 10ml of ternary mixtures of known composition within the two phase region were prepared in vials and were stirred vigorously for 1h and left to settle for 12 h in a thermostatic bath (Lauda E200 water thermostat) at 25 ºC, to ensure complete separation between the two phases. Then, samples from both phases were taken with a syringe and their densities and refractive indices were measured at 298.15 K. In order to not disturb the equilibrium, avoid contamination from one phase with the other, special capped needles were used. The IL rich phase is always denser (bottom phase) than the heptane rich phase (upper phase).

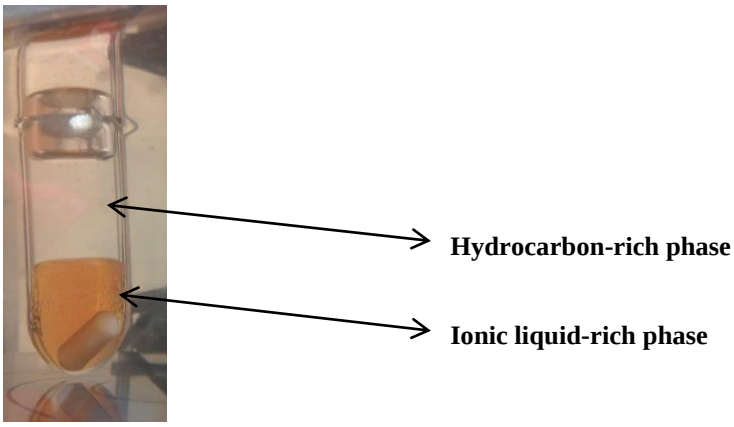

Figure 3.3 Two separate phases of the ternary systems under study for tie-line determination.

Lastly, the phase compositions in equilibrium were inferred by means of calibration curves which were previously constructed at 298.15 K. For this purpose, five ternary mixtures in the one phase region were prepared and their densities and refractive indices measured at 298.15K. The obtained data were correlated using the following equations:

$$\boldsymbol{\rho = Aw_1 + Bw_1^2 + Cw_1^3 + Dw_1^4 + Ew_2 + Fw_2^2 + Gw_2^3 + Hw_2^4 + Iw_3 + Jw_3^2 + Kw_3^3 + Lw_3^4} \quad \textbf{(3.3)}$$

$$\boldsymbol{n_D = Mw_1 + Nw_1^2 + Ow_1^3 + Pw_1^4 + Qw_2 + Rw_2^2 + Sw_2^3 + Tw_2^4 + Uw_3 + Vw_3^2 + Ww_3^3 + Xw_3^4} \quad \textbf{(3.4)}$$

$$\boldsymbol{w_3 = 1 - (w_1 + w_2)} \quad \textbf{(3.5)}$$

where w_1, w_2 and w_3 correspond to the mass fraction of the ionic liquid, heptane and ethanol, respectively, and A to X are adjustable parameters. To measure the difference between the values given by the model and the values actually observed, the root-means-square-deviation (RMSD) was calculated according to the Equation 3.6:

$$\boldsymbol{RMSD = \left(\sum_i^n \frac{(y_{exp} - y_{calc})^2}{n} \right)^{\frac{1}{2}}} \quad \textbf{(3.6)}$$

where y_{exp} and y_{calc} are the experimental and calculated property, respectively, and n is the number of experimental points. Moreover, to validate this method, four mixtures with different compositions were prepared for each system and their densities and refractive indices were measured and compared to those predicted by the proposed Equations 3.3, 3.4 and 3.5. The measurement of the refractive indices took place at atmospheric pressure and 25 ºC through an automated Anton Paar Refractometer Abbemat 500 with an absolute uncertainty of ± 0.0005. Densities were measured by using an Anton Paar DMA 5000 Density Meter (Figure 3.4) with a precision of 10^{-6} g.cm^{-3} and an uncertainty of 3.10^{-5} g.cm^{-3} was obtained.

Figure 3.4 Anton Paar DMA 5000 Density Meter used in this work.

3.3 Results and Discussion

3.3.1 Heptane + Ethanol + [C_2MIM][SCN]

The binodal curve data points for the ternary system heptane + ethanol + [C_2MIM][SCN] at 298.15K and atmospheric pressure are detailed in Table 3.1 and plotted in Figure 3.5. Their corresponding densities and refractive indices are shown in Appendix B (Figure B1). It can be observed that this systems presents a fairly large immiscibility region. Also, the alkane and the ionic liquid are practically immiscible.

Table 3.1 Experimental data in mass fraction (*w*) and molar fraction(*x*) of the binodal curve for the ternary system heptane (1) + ethanol (2) + [C_2MIM][SCN] (3) at 298.15K and atmospheric pressure.

w_1	w_2	w_3	x_1	x_2	x_3
0.0000	0.0000	1.0000	0.0000	0.0000	1.0000
1.0000	0.0000	0.0000	1.0000	0.0000	0.0000
0.0000	1.0000	0.0000	0.0000	1.0000	0.0000
0.9871	0.0129	0.0000	0.9723	0.0277	0.0000
0.9790	0.0210	0.0000	0.9555	0.0445	0.0000
0.9514	0.0486	0.0000	0.9000	0.1000	0.0000
0.9159	0.0841	0.0000	0.8336	0.1664	0.0000
0.8912	0.1064	0.0024	0.7929	0.2059	0.0013
0.8328	0.1633	0.0039	0.6996	0.2984	0.0019
0.7791	0.2167	0.0042	0.6218	0.3762	0.0020
0.7339	0.2583	0.0078	0.5644	0.4321	0.0035
0.6477	0.3297	0.0226	0.4699	0.5204	0.0097
0.5395	0.4161	0.0444	0.3668	0.6154	0.0179
0.4952	0.4478	0.0570	0.3295	0.6481	0.0225
0.3743	0.5231	0.1025	0.2380	0.7234	0.0386
0.3108	0.5556	0.1336	0.1944	0.7561	0.0495
0.2740	0.5710	0.1550	0.1704	0.7725	0.0571
0.2231	0.5818	0.1951	0.1391	0.7889	0.0720
0.1871	0.5851	0.2278	0.1173	0.7981	0.0846
0.1524	0.5868	0.2608	0.0962	0.8062	0.0975
0.1221	0.5724	0.3055	0.0789	0.8043	0.1168
0.1030	0.5588	0.3383	0.0678	0.8003	0.1319
0.0855	0.5369	0.3776	0.0579	0.7907	0.1514
0.0629	0.5144	0.4227	0.0439	0.7813	0.1748
0.0556	0.4972	0.4473	0.0396	0.7714	0.1889
0.0435	0.4740	0.4825	0.0320	0.7580	0.2100
0.0353	0.4504	0.5144	0.0267	0.7425	0.2308
0.0321	0.4256	0.5423	0.0251	0.7238	0.2511
0.0262	0.3606	0.6132	0.0223	0.6683	0.3093
0.0210	0.3226	0.6563	0.0189	0.6314	0.3497
0.0181	0.2791	0.7028	0.0173	0.5831	0.3996
0.0137	0.2361	0.7502	0.0141	0.5287	0.4572
0.0120	0.1947	0.7933	0.0133	0.4678	0.5189
0.0111	0.1319	0.8570	0.0138	0.3563	0.6299
0.0099	0.0816	0.9085	0.0137	0.2447	0.7416

In Table 3.2 the fitting parameters of equations 3.3 and 3.4 together with the RMSD. The Pearson correlation coefficient was also calculated to measure the linear correlation between y_{exp} and y_{calc} giving a value between -1 and +1. The PCC displays a value very close to +1, meaning that there is practically a perfect correlation between the two variables. The application of the mathematical software *Solver* allowed the minimization of the RMSD by altering the adjustable parameters from A to X. The uncertainty in the phase composition was estimated to be ± 0.0075 in mass fraction.

Table 3.2 Fitting parameters (A to X) of the density (ρ) and refractive indices (n_D) of equations 3.1 and 3.2 , root-mean-square deviation (RMSD) and Pearson Correlation Coefficient (PCC) for the system heptane + ethanol + [C_2MIM][SCN].

	Property			
$\boldsymbol{\rho}$	$A = 0.90710$	$B = 1.34589$	$C = -1.48509$	$D = 0.34522$
	$E = 0.89704$	$F = -0.07960$	$G = 0.15437$	$H = -0.24020$
	$I = 0.16066$	$J = 0.91213$	$K = 0.31998$	$L = -0.61118$
	n = 35	**RMSD = 0.00095**		**PCC = 0.99995**
$\boldsymbol{n_D}$	$M = 2.08330$	$N = -0.76648$	$O = 0.34975$	$P = -0.11733$
	$Q = 1.39072$	$R = 1.04187$	$S = -1.67397$	$T = 0.62613$
	$U = 0.90560$	$V = 0.39267$	$W = 0.05231$	$X = 0.00676$
	n = 35	**RMSD = 0.00085**		**PCC = 0.99972**

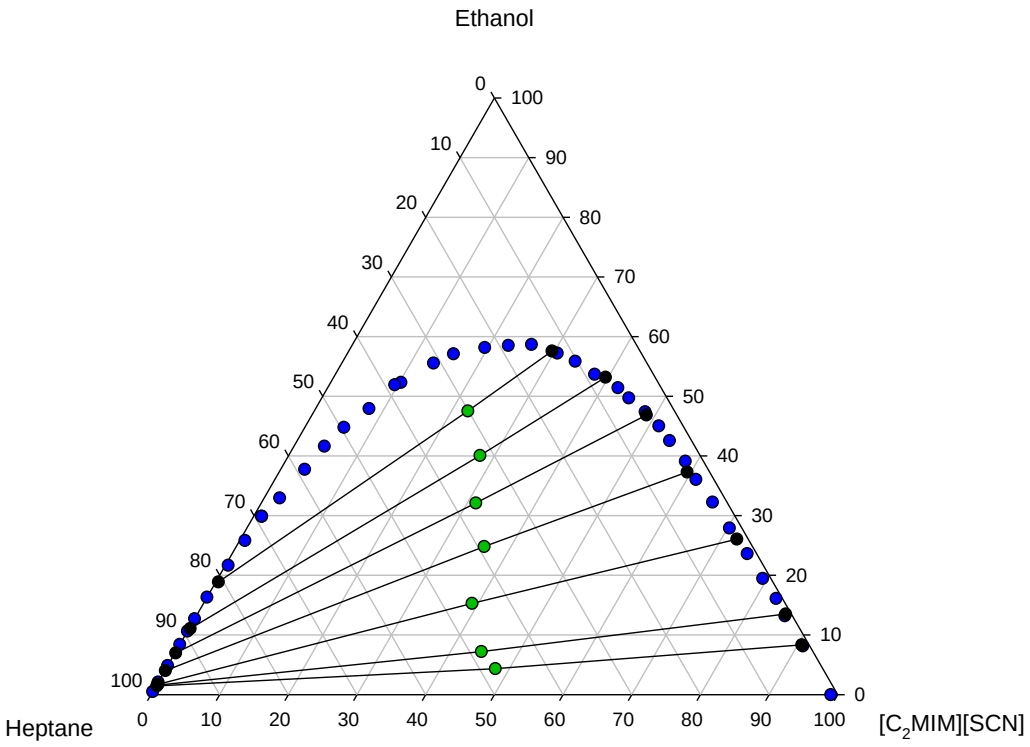

Figure 3.5 Ternary diagram for the system heptane + ethanol + [C_2MIM][SCN] at 298.15 K and atmospheric pressure. The blue dots represent the composition of the experimental binodal curve, the green dots the initial composition of the ternary mixture and the black dots the composition of the two phases in equilibrium. The lines connecting the composition of the two phases in equilibrium are the system tie-lines.

Seven ternary mixtures within the two phase region were prepared and the composition of the phases in equilibrium determined as described before. These experimental results for the liquid-liquid extractions of ethanol from the heptane + ethanol azeotrope with the pure ionic liquid [C_2MIM][SCN] at 298.15K and atmospheric pressure are presented in Table 3.3.

Table 3.3 Composition (*w* denotes mass fraction) of the experimental phase in equilibrium for the ternary system heptane (1) + ethanol (2) + [C_2MIM][SCN] (3) at 298.15K and atmospheric pressure.

Starting point			**Heptane-rich phase**		**IL-rich phase**	
w_1	w_2	w_3	w_1	w_2	w_1	w_2
0.4768	0.0436	0.4796	0.9867	0.0124	0.0108	0.0836
0.4827	0.0722	0.4450	0.9856	0.0135	0.0082	0.1349
0.4559	0.1530	0.3911	0.9839	0.0148	0.0165	0.2605
0.3906	0.2482	0.3612	0.9608	0.0384	0.0327	0.3729
0.3663	0.3212	0.3124	0.9301	0.0689	0.0443	0.4685
0.3204	0.4008	0.2788	0.8876	0.1105	0.0721	0.5319
0.3009	0.4753	0.2238	0.8072	0.1888	0.1276	0.5757

3.3.2 Heptane + Ethanol +$[C_2MIM][SCN]_{0.9}[C_2SO_4]_{0.1}$

The second solvent studied for the LLE of ethanol from heptane + ethanol system was a mixture of ILs, more precisely $[C_2MIM][SCN]_{0.9}[C_2SO_4]_{0.1}$. The experimental data of the binodal curve is shown in Table 3.4. The ternary diagram with the tie-lines for the system heptane + ethanol + $[C_2MIM][SCN]_{0.9}[C_2SO_4]_{0.1}$ is plotted in Figure 3.6 where it can be observed that the immiscibility area is practically identical to the heptane + ethanol + $[C_2MIM][SCN]$, which is reasonable, since the mixture is composed of only 10% in mass of a different ionic liquid. Table 3.5 shows the fitting parameters of Equations 3.3 and 3.4 together with the RMSD as well as the PCC.

Table 3.4 Experimental data in mass fraction (w) and molar fraction(x) of the binodal curve for the ternary system heptane (1) + ethanol (2) +$[C_2MIM][SCN]_{0.9}[C_2SO_4]_{0.1}$ (3) at 298.15K and atmospheric pressure.

w_1	w_2	w_3	x_1	x_2	x_3
0.0000	0.0000	1.0000	0.000	0.0000	1.0000
1.0000	0.0000	0.0000	1.0000	0.0000	0.0000
0.0000	1.0000	0.0000	0.0000	1.0000	0.0000
0.9901	0.0099	0.0000	0.9788	0.0212	0.0000
0.9878	0.0122	0.0000	0.9739	0.0261	0.0000
0.9705	0.0295	0.0000	0.9380	0.0620	0.0000
0.9515	0.0485	0.0000	0.9002	0.0998	0.0000
0.9121	0.0879	0.0000	0.8266	0.1734	0.0000
0.8481	0.1519	0.0000	0.7196	0.2804	0.0000
0.7999	0.2001	0.0000	0.6475	0.3525	0.0000
0.7449	0.2486	0.0064	0.5779	0.4196	0.0025
0.6925	0.2964	0.0111	0.5158	0.4801	0.0041
0.6533	0.3266	0.0200	0.4756	0.5172	0.0072
0.6008	0.3680	0.0311	0.4241	0.5651	0.0109
0.5211	0.4237	0.0551	0.3545	0.6270	0.0185
0.4500	0.4703	0.0797	0.2975	0.6764	0.0260
0.4021	0.5011	0.0968	0.2611	0.7078	0.0311
0.3456	0.5316	0.1228	0.2212	0.7400	0.0388
0.3233	0.5442	0.1325	0.2056	0.7528	0.0416
0.2889	0.5654	0.1458	0.1816	0.7731	0.0453
0.2535	0.5763	0.1702	0.1593	0.7878	0.0529
0.2275	0.5860	0.1865	0.1427	0.7995	0.0578
0.2064	0.5896	0.2040	0.1298	0.8068	0.0634
0.1862	0.5876	0.2262	0.1182	0.8109	0.0709
0.1673	0.5837	0.2490	0.1072	0.8139	0.0789
0.1422	0.5826	0.2752	0.0920	0.8200	0.0880
0.1278	0.5769	0.2953	0.0836	0.8209	0.0954
0.1105	0.5611	0.3284	0.0740	0.8173	0.1087
0.0847	0.5332	0.3820	0.0591	0.8092	0.1317
0.0674	0.5110	0.4216	0.0486	0.8012	0.1502
0.0513	0.4868	0.4619	0.0383	0.7911	0.1706
0.0444	0.4596	0.4960	0.0344	0.7755	0.1901
0.0395	0.4358	0.5247	0.0317	0.7603	0.2080
0.0303	0.3950	0.5747	0.0259	0.7321	0.2420
0.0222	0.3401	0.6376	0.0206	0.6869	0.2925
0.0134	0.2950	0.6916	0.0134	0.6437	0.3428
0.0063	0.2483	0.7454	0.0069	0.5904	0.4027
0.0000	0.1805	0.8195	0.0000	0.5078	0.4922
0.0000	0.0971	0.9029	0.0000	0.6787	0.3213

Table 3.5 Fitting parameters (A to X) root-mean-square deviation (RMSD) and Pearson Correlation Coeffient (PCC) for the system heptane + ethanol + $[C_2MIM][SCN]_{0.9}[C_2SO_4]_{0.1.}$

	Property			
$\boldsymbol{\rho}$	$A = 1.07555$	$B = 0.10793$	$C = 0.09614$	$D = -0.16049$
	$E = 0.68376$	$F = 0.01387$	$G = 0.08516$	$H = -0.10345$
	$I = 0.63987$	$J = 0.30882$	$K = -0.19335$	$L = 0.02623$
	n = 35	**RMSD = 0.00073**		**PCC = 0.99996**
$\boldsymbol{n_D}$	$M = 1.53614$	$N = 0.11078$	$O = -0.04376$	$P = -0.05419$
	$Q = 1.35201$	$R = 0.27617$	$S = -0.24421$	$T = 0.00156$
	$U = 1.13532$	$V = 0.50663$	$W = -0.24688$	$X = -0.03767$
	n = 35	**RMSD = 0.00101**		**PCC = 0.99922**

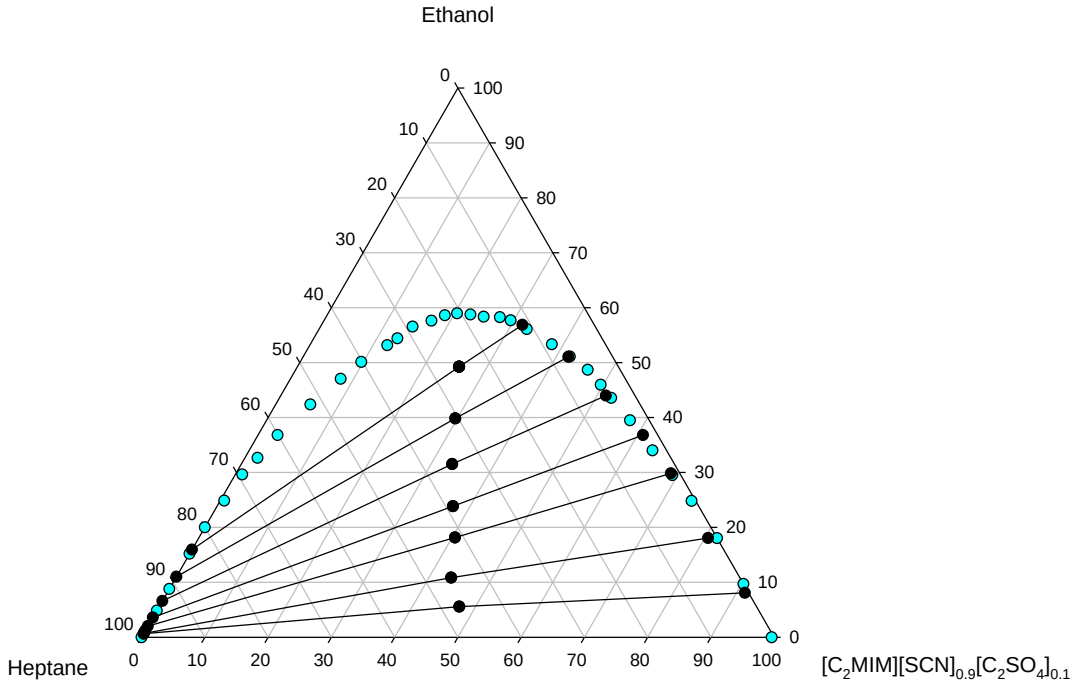

Figure 3.6 Triangular diagram for the system heptane + ethanol + ($[C_2MIM][SCN]$ + $[C_2MIM][C_2SO_4]$) at 298.15 K. The cyan dots represent the binodal curve and the black dots and lines the system tie-lines and starting point mixtures.

The experimental results for the liquid-liquid extractions of ethanol from the heptane + ethanol azeotrope with the ionic liquid mixture are presented in Table 3.6.

Table 3.6 Composition of the experimental tie-line ends, solute distribution ratio (β) and selectivity (S) for the ternary system [C_2MIM][SCN]+[C_2MIM][C_2SO_4] at 298.15 K.

Starting point			Heptane-rich phase		IL-rich phase	
w_1	w_2	w_3	w_1	w_2	w_1	w_2
0.4697	0.0558	0.4745	0.9941	0.0065	0.0059	0.0808
0.4562	0.1086	0.4351	0.9931	0.0069	0.0116	0.1806
0.4136	0.1815	0.4049	0.9796	0.0203	0.0134	0.2985
0.3885	0.2385	0.3730	0.9640	0.0361	0.0224	0.3680
0.3511	0.3154	0.3335	0.9342	0.0661	0.0441	0.4400
0.3048	0.3984	0.2968	0.8900	0.1103	0.0674	0.5107
0.2516	0.4924	0.2560	0.8410	0.1595	0.1109	0.5687

3.3.3. Selectivity and Distribution Coefficient

The experimental results for the extraction of ethanol from heptane +ethanol azeotropic mixture using either the pure [C_2MIM][SCN] IL and the [C_2MIM][SCN]$_{0.9}$[C_2SO_4]$_{0.1}$ IL mixture are presented in Table 3.7. The distribution coefficient and selectivity for pure [C_2MIM][SCN] IL and the [C_2MIM][SCN]$_{0.9}$[C_2SO_4]$_{0.1}$ IL mixture, calculated using Equation 3.1 and Equation 3.2, respectively, are also presented.

Table 3.7 Composition of the two phases in equilibrium, solute distribution ratio (β) and selectivity (S) for the ternary systems heptane (1) + ethanol (2) + [C_2MIM][SCN] (3) or [C_2MIM][SCN]$_{0.9}$[C_2SO_4]$_{0.1}$ (3) at 298.15 K.

{Azeotrope + [C_2MIM][SCN]}					
Heptane-rich phase		IL-rich phase			
w_1	w_2	w_1	w_2	β	S
0.9867	0.0124	0.0108	0.0836	6.76	619.97
0.9856	0.0135	0.0082	0.1349	10.00	1200.05
0.9839	0.0148	0.0165	0.2605	17.56	1044.14
0.9608	0.0384	0.0327	0.3729	9.71	285.45
0.9301	0.0689	0.0443	0.4685	6.80	142.65
0.8876	0.1105	0.0721	0.5319	4.81	59.23
0.8072	0.1888	0.1276	0.5757	3.05	19.29
{Azeotrope + ([C_2MIM][SCN]+[C_2MIM][C_2SO_4] }					
w_1	w_2	w_1	w_2	β	S
0.9941	0.0065	0.0059	0.0808	12.40048	2089.391
0.9931	0.0069	0.0116	0.1806	26.17391	2236.925
0.9796	0.0203	0.0134	0.2985	14.69454	1073.226
0.9640	0.0361	0.0224	0.3680	10.20797	439.8677
0.9342	0.0661	0.0441	0.4400	6.661199	141.047
0.8900	0.1103	0.0674	0.5107	4.631896	61.14495
0.8410	0.1595	0.1109	0.5687	3.564753	27.04155

The values of the distribution coefficient and selectivities as a function of the ethanol in the hydrocarbon-rich phase are shown in Figure 3.7 and Figure 3.8, respectively, allowing a direct comparison between the two systems studied.

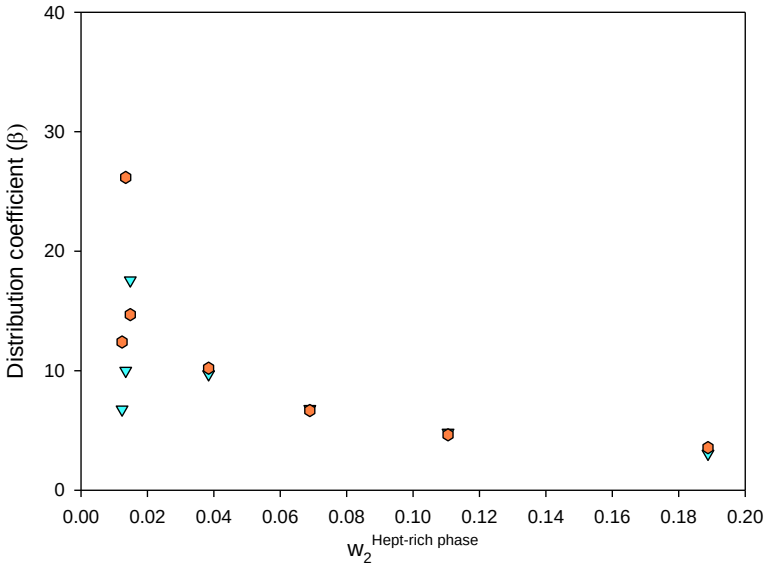

Figure 3.7 Distribution coefficients (β) for the ternary systems heptane + ethanol + IL at T=298.15 K: (▼) $[C_2MIM][SCN]$ (●) $[C_2MIM][SCN]+[C_2MIM][C_2SO_4]$.

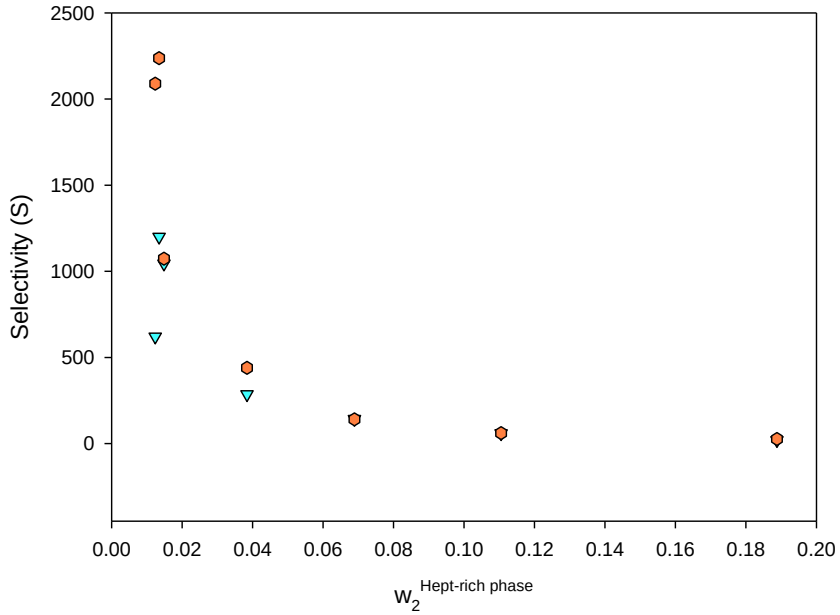

Figure 3.8 Selectivity (S) of (▼) $[C_2MIM][SCN]$ (●) $[C_2MIM][SCN]_{0.9}[C_2SO_4]_{0.1}$ for the liquid-liquid extraction of ethanol from heptane + ethanol system at T=298.15 K and atmospheric pressure.

By analysing Table 3.7 and Figures 3.7 and 3.8 it can be observed that the $[C_2MIM][SCN]_{0.9}[C_2SO_4]_{0.1}$ presents a selectivity and a distribution coefficient approximately

twice as high as the pure $[C_2MIM][SCN]$ IL, at an ethanol mass fraction approximately between 0.7 and 1.3% in the hydrocarbon-rich phase. These values clearly show that the IL mixture is more capable of extracting the ethanol from the heptane + ethanol azeotrope than the pure ionic liquid. Consequently, a lower solvent flow rate would be required if the $[C_2MIM][SCN]_{0.9}[C_2SO_4]_{0.1}$ was chosen and its higher affinity to the solute implies that more ethanol is drawn to the extract phase, consequently leading to a more pure raffinate ($w_1^{Heptane-rich\ phase} = 0.9867$ for $[C_2MIM][SCN]$; $w_1^{Heptane-rich\ phase} = 0.9941$ for $[C_2MIM][SCN]_{0.9}[C_2SO_4]_{0.1}$). Moreover, the fact that the IL mixture is twice as selective as $[C_2MIM][SCN]$ at the referred concentration of solute, shows that it has a greater extraction power, meaning that the extraction unit would need fewer equilibrium stages in the process and fewer amounts of inert residual would be present in the extract. Therefore, maximum extraction is achieved when there is about 1%wt of the solute in the heptane-rich phase, and a decrease is observed as more ethanol is present in the hydrocarbon-rich phase. This decrease is more noticeable at low concentrations of the alcohol in the upper phase and, as a result, the extraction of the solute towards the ionic liquid-rich phase is more favourable at low concentrations of ethanol.

3.4 Comparison to Other Solvents

The $[C_2MIM][SCN]_{0.9}[C_2SO_4]_{0.1}$ IL mixture studied in this work consisted of $[C_2MIM][SCN]$ and $[C_2MIM][C_2SO_4]$. This last IL was chosen due to its relatively low cost, compared to some other sulfate based ILs (such as $[C_1MIM][C_1SO_4]$), which would be of interest when considering a possible scale-up study. It was shown previously in this study that mixing $[C_2MIM][C_2SO_4]$ IL significantly increased the extraction efficiency of using pure $[C_2MIM][SCN]$ IL to break the azeotrope heptane + ethanol, not to mention the production of a purer raffinate. Figures 3.9 and Figure 3.10 show a comparison between the three solvents involved that could be used as extraction agents in this process in terms of selectivity (S) and distribution coefficient (β), respectively.

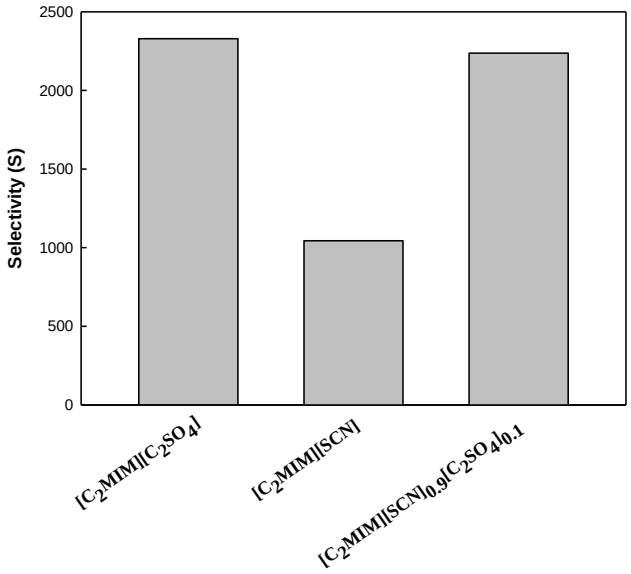

Figure 3.9 Selectivity, S, of the system with the azeotrope heptane + ethanol at an ethanol mass fraction of approx. 1 % *wt* in heptane-rich phase at 25 ^{0}C.

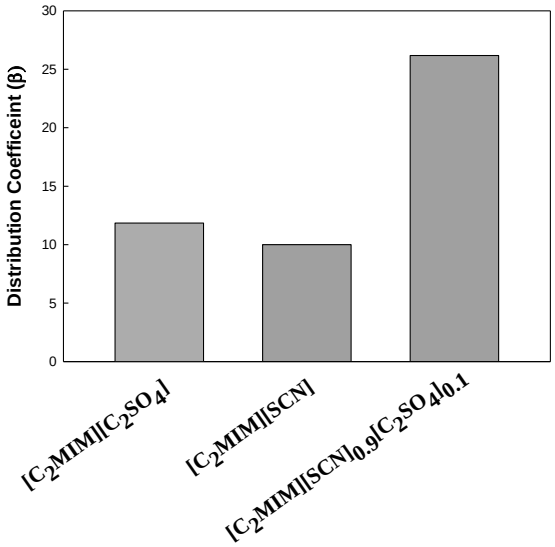

Figure 3.10 Distribution coefficient (β) of the system with the azeotrope heptane + ethanol at an ethanol mass fraction of approx. 1 % *wt* in heptane-rich phase at 25 ºC.

Comparing the above figures, it is possible to conclude that pure $[C_2MIM][C_2SO_4]$ as the azeotrope breaker is slightly more selective than both the pure $[C_2MIM][SCN]$ and the $[C_2MIM][SCN]_{0.9}[C_2SO_4]_{0.1}$ IL mixture, when there is 1 % wt of ethanol in the heptane-rich phase. However, for the same alcohol mass percentage in the hydrocarbon-rich phase, the ionic

liquid mixture has twice the solute-carrying capacity (justified by the values of β) than the pure $[C_2MIM][C_2SO_4]$ ionic liquid. This means that, in an extraction unit, a lower solvent flow rate would be necessary if the ionic liquid mixture was chosen, whereas choosing the pure $[C_2MIM][C_2SO_4]$ would lead to fewer equilibrium stages in the process.

A comparison in terms of selectivity and distribution coefficient was also made with other ILs studied in the breaking of this azeotrope. Figures 3.11 and 3.12 illustrate this comparison.

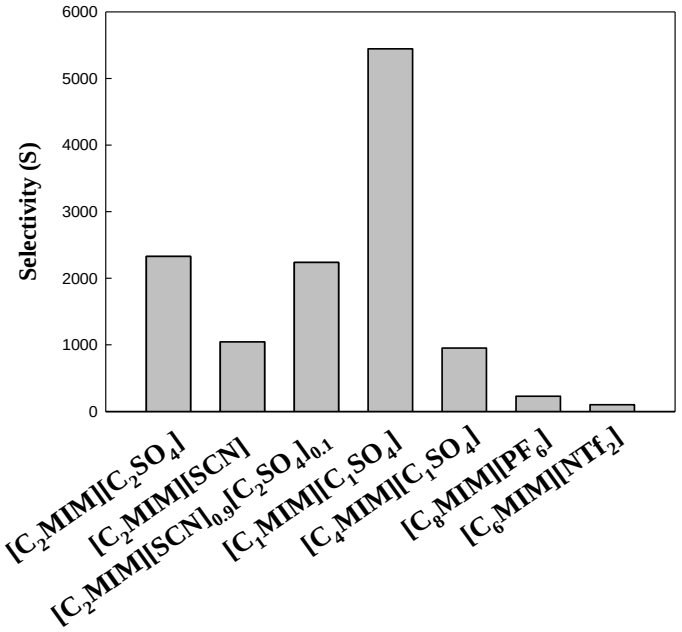

Figure 3.11 Selectivities for various ILs studied as solvents for the separation of the azeotrope heptane + ethanol at an ethanol mass fraction of approx. 1 % *w*t in heptane-rich phase at 25 ^{0}C.

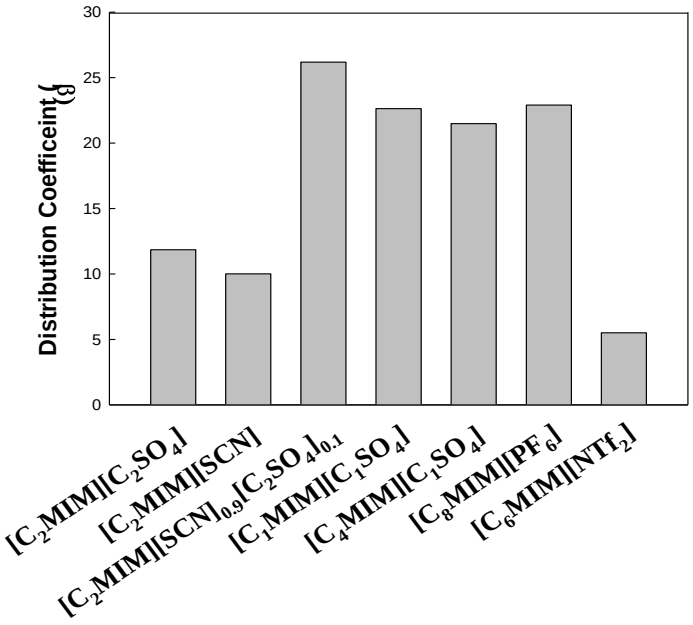

Figure 3.12 Distribution coefficients (β) for various ILs studied as solvents for the separation of the azeotrope heptane + ethanol at an ethanol mass fraction of approx. 1 % wt in heptane-rich phase at 25 ºC.

From the analysis of the above figures, it is possible to observe that the $[C_2MIM][SCN]_{0.9}[C_2SO_4]_{0.1}$ is more selective than most of other ILs studied, with the exception of pure $[C_1MIM][C_1SO_4]$. It was possible to confirm that, as literature showed[3] the presence of a shorter alkyl chain in the imidazolium leads to a higher selectivity. The mixture studied in this dissertation shows the highest distribution coefficient out of the ILs studied referred (Figure 3.12). It can be interpreted that the presence of the specific proportion of $[C_2MIM][C_2SO_4]$ in the mixture is likely to play an important role in terms of solute-carrying capacity of the solvent, where the sulfate anion can form stronger hydrogen bonding interactions with the ethanol than the other ILs. However, the fact that the solvent is composed mainly of $[C_2MIM][SCN]$ may also be behind the explanation in a somewhat subtle way. It was already established that the solvent has a greater ionicity than pure $[C_2MIM][SCN]$, approaching the behaviour of the ideal electrolyte. This means than ions present in the system are less coordinated and more "free" to establish the possible interactions with the components involved. The thiocyanate anion is mainly responsible for the conduction process (pure $[C_2MIM][SCN]$ has a high ion conductivity already) and is less likely to form H-bonds with the ethanol than the sulfate anion (oxygen is more electronegative than nitrogen). Therefore, the sulfate anion is more "free" to establish strong hydrogen bonds with the solute, consequently, justifying the enormous increase in the distribution coefficient.

4. Final Remarks

4.1 Conclusions and Future Work

The main goal of this work was to study the possibility of a relationship between the extraction efficiency of breaking the azeotropic mixture heptane + ethanol and the ionicity of the solvent used for the process. For this particular system, it was demonstrated that increasing the ionicity of the pure ionic liquid 1-ethyl-3-methylimidazolium thiocyanate [C_2MIM][SCN] by dissolving 1-ethyl-3-methylimidazolium ethyl sulfate [C_2MIM][C_2SO_4] in a certain molar composition led to a more efficient and selective extraction of the alcohol. The selectivity (S) and solute distribution ratio (β) were observed to be about twice as high as when choosing the pure ionic liquid as a solvent. Taking into account that the concept of ionicity is related to the ions available to participate in conduction and the fluidity of the system it may be reasonable to assume that the breaking of the azeotrope is more effective, since more "free ions" are present to establish interactions with the solute. A reduced ionicity increases the likelihood of the formation of complex aggregates, therefore preventing the interaction with the ethanol.

This thesis also permitted to demonstrate the ability of an ionic liquid as a solvent for the separation of azeotropes by liquid-liquid extraction. The design of any extraction process should be addressed on the basis of the following points: i) determination of LLE data for the ternary systems, ii) correlation of the experimental data by means of polynomial equations, iii) evaluation the extraction capacity with crucial parameters such as the distribution coefficients and selectivities. It can be concluded that thiocyanate based ILs can be a promising alternative to conventional solvents as they possess a high ionicity compared with many other ILs and, in case of the particular ternary system studied in this work, allow a raffinate purity of over 98 % *w*t, as shown by the experimental LLE data. The best candidate, however, is the High Ionicity Ionic Liquid ([C_2MIM][SCN]+[C_2MIM][C_2SO_4]) in the well-defined proportions as they present the highest selectivity values and distribution coefficients, as well as permitting a raffinate purity of over 99% *w*t. To sum up, the use of ILs as azeotrope breakers should help relief the increasing concern about environmental issues, as well as the establishment of new regulations.

As future work, it would be interesting to conduct a study based on the possibility of a scale-up to an industrial level, which would involve the dimensioning of a liquid-liquid extraction column as well a simulation and optimization of the process. Taking into consideration that a raffinate of heptane with a purity of over 99 % *w*t was achieved, scaling-up for an industrial application seems motivating.

A different and important study of the feasibility of this project would be to involve, in more detail, economic aspects in the design of the process and compare it with typical separation processes, such as extractive/azeotropic distillation. The fact remains that a simple distillation would always be necessary to recover the ethanol dissolved in the ionic liquid, so that it could be reused. Nevertheless, the issue of the energy costs associated with reaching a single fluid phase system would cease to exist in the liquid-liquid extraction column, which takes place at room temperature and atmospheric pressure.

5. References

[1] Hilmen, Eva-Katrine, Separation of Azeotropic Mixtures:Tools for Analysis and Studieson Batch Distillation Operation A Thesis Submitted for the Degree of Dr. Ing.Norwegian University of Science and Technology Department of Chemical Engineering November 2000

[2] Moore, Walter J. Physical Chemistry, 3rd ed., Prentice-Hall 1962, pp. 140–142
'CRC Handbook of Chemistry and Physics', ed. D. R. Lide, CRC
Press, Boca Raton, 73rd edn., 1992

[3] Pereiro, A. B, et al., *Ionic liquids in separations of azeotropic systems – A review, 2011*

[4] Rogers, R.D, et al., Ionic Liquids – Industrial Applications to Green

Chemistry, ACS Symposium Series 818, Washington, DC, American Chemical Society, 2002.

[5] Plechkova, N.V. et.al., Chem. Soc. Rev. 37 (2008) 123–150

[6] Huddleston, J.G., et al., Green Chem. 3 (2001) 156–164

[7] Earle, M.J., et, al., Nature 439 (2006) 831–834.

[8] Smiglak, W.M., et al., Chem. Commun. 24 (2006) 2554–2556.

[9] Petkovic, M., Chem. Soc. Rev. 40 (2011) 1383–1403.

[10] Welton, T., *Room-Temperature Ionic Liquids. Solvents for Synthesis and Catalysis* Department of Chemistry, Imperial College of Science Technology and Medicine, South Kensington, London SW7 2AY, U.K]

[11] Natalia V. Plechkovaa and Kenneth R. Seddon *Applications of ionic liquids in the chemical industry* Received 28th August 2007. First published as an Advance Article on the web 30th November 2007 DOI: 10.1039/b006677j

[12] W. Arlt, M. Seiler, C. Jork and T. Schneider, *Ionic liquids as selective additives for the separation of close-boiling or azeotropic mixtures,* World Pat., WO 2002 074718 (2002).

[13] IFP, 'Annual Report', 2004.

[14] Y. Chauvin, J. F. Gaillard, D. V. Quang and J. W. Andrews, *Chem. Ind*., 1974, 375–378.

[15] Heiko Niedermeyer, Jason P. Hallett, Ignacio J. Villar-Garcia, Patricia A. Hunt and Tom Welton, *Mixtures of ionic liquids*, received 11th May 2012, DOI: 10.1039/c2cs35177c

[16] K. Tominaga, *Catal. Today*, 2006, 115, 70.
[17] A. S.Best,A. I.Bhatt and A. F. Hollenkamp, *J. Electrochem. Soc*., 2010, 157, A903.

[18] M.J. Earle, J.M.S.S. Esperanca, M.A. Gilea, J.N.C. Lopes, L.P.N. Rebelo, J.W. Magee, K.R. Seddon, J.A. Widegren, Nature 439 (2006) 831–834.

[19] A. B. Pereiro, J. M. M. Araújo, J. M. S. S. Esperança, I. M. Marrucho and L. P. N. Rebelo, *J. Chem. Thermodyn*., 2012, 46, 2–28.

[20] Ana B. Pereiro and Ana Rodriguez *Separation of Ethanol-Heptane Azeotropic Mixtures by Solvent Extraction with an Ionic Liquid*, Ind. Eng. Chem. Res. 2009, 48, 1579–1585

[21] Filipe S. Oliveira, Ana B. Pereiro, Luís P. N. Rebelo and Isabel M. Marrucho, *Deep eutectic solvents as extraction media for azeotropic mixtures*, Green Chem., 2013, 15, 1326

[22] S.J. Marwil, Separation of hydrocarbon and alcohol azeotropic mixtures by distillation with anhydrous ammonia, US Patent 4437941, 1984.

[23] T. Okada, T. Matsuura, in: Proc. Int. Conf. Pervaporation Processes Chem. Ind. 3 (1988) 224-230.

[24] M. Laatikainen, M. Lindstrom, Acta Polytech Scand., Chem. Tech. Metall.Series 175 (1986) 1–61.

[25] T.M. Letcher, N. Deenadayalu, B. Soko, D. Ramjugernath, P.K. Naicker, J. Chem. Eng. Data 48 (2003) 904–907

[26] A.B. Pereiro, F.J. Deive, J.M.S.S. Esperanca, A. Rodriguez, Fluid Phase Equilib. 291 (2010) 13–17

[27] U. Domanska, Z. Zolek-Tryznowska, A. Pobudkowska, J. Chem. Eng. Data 54 (2009) 972–976

[28] A.B. Pereiro, A. Rodriguez, Green Chem. 11 (2009) 346–350

[29] A.B. Pereiro, A. Rodriguez, Chem. Eng. J. 153 (2009) 80–85.

[30] A.B. Pereiro, A. Rodriguez, Fluid Phase Equilib. 270 (2008) 23–29.

[31] A.B. Pereiro, A. Rodriguez, Ind. Eng. Chem. Res. 48 (2009) 1579–1585.

[32] A.B. Pereiro, A. Rodriguez, Sep. Purif. Technol. 62 (2008) 733–738.~

[33] A.B. Pereiro, E. Tojo, A. Rodriguez, J. Canosa, J. Tojo, Green Chem. 8 (2006) 307–310.

[34] A.B. Pereiro, A. Rodriguez, Applications of ionic liquids in azeotropic mixtures

separations, in: A. Kokorin (Ed.), Ionic Liquids, Applications and Perspectives, INTECH, Rijeka, Croatia, 2011, pp. 225–242.
[35] Filipe S. Oliveira, et al. *High Ionicity Ionic Liquids (HIILs): Comparing Ethylsulfonate and Ethylsulfate Anion Effect*, PCCP, DOI: 10.1039/c0xx00000x

[36] Douglas R. MacFarlane et al. *On the concept of ionicity in ionic liquids*, PCCP, DOI: 10.1039/b900201d

[37] Ana B. Pereiro et al. *Inorganic salts in purely ionic liquid media: the development of high ionicity ionic liquids (HIILs)*, Chem. Commun., 2012, **48**, 3656–3658

[38] A.B. Pereiro, J.M.M. Araújo, F.S. Oliveira, J.M.S.S. Esperança, J.N. Canongia Lopes, I.M. Marrucho, L.P.N. Rebelo, *Solubility of inorganic salts in pure ionic liquids*, J. Chem. Thermodynamics 55 (2012) 29–36

[39] C. A. Angell, N. Byrne and J.-P. Belieres, Acc. Chem. Res., 2007,40, 1228.

[40]W. Xu, E. I. Cooper and C. A. Angell, J. Phys. Chem. B, 2003, 107,6170–6178.

[41] M. Yoshizawa, W. Xu and C. A. Angell, J. Am. Chem. Soc., 2003,125, 15411–15419

[42] E.J. Gonzalez, N. Calvar, E. Gomez, A. Dominguez, J. Chem. Eng. Data 55 (2010) 3422–3427.

[43] A. Arce, H. Rodriguez, A. Soto, Green Chem. 9 (2007) 247–253.

[44] Y. Umebayashi, T. Mitsugi, S. Fukuda, T. Fujimori, K. Fujii, R.Kanzaki, M. Takeuchi and S.-I. Ishiguro, *J. Phys. Chem. B*, 2007, 20 **111**, 13028-13032.

[45] Y. Umebayashi, S. Mori, K. Fujii, S. Tsuzuki, S. Seki, K. Hayamizu and S.-i. Ishiguro, *J. Phys. Chem. B*, 2010, **114**, 6513-6521.

[46] Q. Zhou, P. D. Boyle, L. Malpezzi, A. Mele, J.-H. Shin, S. Passerini and W. A. Henderson, *Chem. Mater.*, 2011, **23**, 4331-4337.

[47] Karina Shimizu, M. Tariq, Luís P.N. Rebelo, José N. Canongia Lopes, Binary mixtures of ionic liquids with a common ion revisited: A molecular dynamics simulation study, Journal of Molecular Liquids 153 (2010) 52–56

[48] Zuber, Andre, et al., *Thermodynamic Modeling of Ternary Liquid-Liquid Systems with Forming Immiscibility Islands*, Brazilian Archives of Biology and Technology, An International Journal

[49] Treybal, R.E., "Mass Transfer Operations"McGraw Hill Inc.,Tokyo, Japão, 1981.

[50] Wankat, P.C.,"Equilibrium Staged Separations", Blackie Academic & Professional, Glasgow, UK, 1990

Appendix A

Table A1 Fitted parameters of the linear expression given by Equation 2.2

Ionic Liquid Sample	b x 10^{-4}	a	r^2
$[C_2MIM]SCN]$	-5.92	1.2922	0.9999
$[C_2MIM]$ $[SCN]_{0.9610}[NH_4][SCN]_{0.0390}$	-5.97	1.2940	0.9999
$[C_2MIM]$ $[SCN]_{0.9010}[NH_4][SCN]_{0.0990}$	-5.82	1.2902	0.9999
$[C_2MIM]$ $[SCN]_{0.8605}$ $[NH_4][SCN]_{0.1395}$	-5.77	1.2877	0.9998

Table A2 Fitted parameters of the linear expression given by Equation 2.3

Ionic Liquid Sample	$\ln(\eta_0)$	-Ea/R	-Ea/ $kJmol^{-1}$	r^2
$[C_2MIM]$ $[SCN]$	-5.47	2475	20.5	0.9916
$[C_2MIM]$ $[SCN]_{0.9610}[NH_4][SCN]_{0.0390}$	-4.44	2578	21.4	0.9912
$[C_2MIM]$ $[SCN]_{0.9010}[NH_4][SCN]_{0.0990}$	-3.96	2646	21.9	0.9910
$[C_2MIM][SCN]_{0.8605}$ $[NH_4][SCN]_{0.1395}$	-2.11	2891	24.0	0.9902

Table A3 Fitted parameters of the linear expression given by Equation 2.3

Ionic Liquid Sample	$\ln(\sigma_0)$	-Ea/R	-Ea/ $Jmol^{-1}$ ($x10^{-3}$)	r^2
$[C_2MIM]$ $[SCN]$	32.24	0.025	0.207	0.9984
$[C_2MIM]$ $[SCN]_{0.9610}[NH_4][SCN]_{0.0390}$	28.91	0.026	0.216	0.9988
$[C_2MIM]$ $[SCN]_{0.9010}[NH_4][SCN]_{0.0990}$	23.12	0.028	0.232	0.9987
$[C_2MIM]$ $[SCN]_{0.8605}$ $[NH_4][SCN]_{0.1395}$	19.84	0.039	0.324	0.9986

Table A4 Fitted parameters of the linear expression given by Equation 2.2

Ionic Liquid Sample	b x 10^{-4}	a	r^2
$[C_2MIM]$ $[SCN]_{0.7603}[DCA]_{0.2397}$	-6.00	1.2909	0.9999
$[C_2MIM]$ $[SCN]_{0.51120}[DCA]_{.4888}$	-6.15	1.2918	0.9999
$[C_2MIM][SCN]_{0.2585}[DCA]_{0.7415}$	-6.27	1.2914	0.9999

Table A5 Fitted parameters of the linear expression given by Equation 2.3

Ionic Liquid Sample	$\ln(\eta_0)$	-Ea/R	-Ea/ $kJmol^{-1}$	r^2
$[C_2MIM]$ $[SCN]_{0.7603}[DCA]_{0.2397}$	-6.17	2406	20.0	0.9915
$[C_2MIM]$ $[SCN]_{0.5112}[DCA]_{0.4888}$	-6.51	2357	19.5	0.9916
$[C_2MIM]$ $[SCN]_{0.2585}[DCA]_{0.7415}$	-7.96	2265	18.8	0.9919

Table A6 Fitted parameters of the linear expression given by Equation 2.3

Ionic Liquid Sample	$\ln(\sigma_0)$	-Ea/R	-Ea/ $Jmol^{-1}$ ($x10^{-3}$)	r^2
$[C_2MIM]$ $[SCN]_{0.7603}[DCA]_{0.2397}$	33.20	0.024	0.20	0.9988
$[C_2MIM]$ $[SCN]_{0.5112}[DCA]_{0.4888}$	34.43	0.024	0.20	0.9985
$[C_2MIM]$ $[SCN]_{0.2585}[DCA]_{0.7415}$	36.26	0.023	0.19	0.9986

Table A7 Fitted parameters of the linear expression given by Equation 2.2

Ionic Liquid Sample	b x 10^{-4}	a	r^2
$[C_2MIM]$ $[SCN]_{0.8990}$ $[C_2SO_4]_{0.1010}$	-6.16	1.3174	0.9999
$[C_2MIM]$ $[SCN]_{0.6700}[C_2SO_4]_{0.3300}$	-6.12	1.3501	0.9999
$[C_2MIM]$ $[SCN]_{0.3200}[C_2SO_4]_{0.6800}$	-6.29	1.4018	0.9999
$[C_2MIM][C_2SO_4]$	-6.59	1.4349	0.9999

Table A8 Fitted parameters of the linear expression given by Equation 2.3

Ionic Liquid Sample	$\ln(\eta_0)$	-Ea/R	-Ea/ $kJmol^{-1}$	r^2
$[C_2MIM]$ $[SCN]_{0.8990}$ $[C_2SO_4]_{0.1010}$	-6.28	2479	20.6	0.9911
$[C_2MIM]$ $[SCN]_{0.6700}[C_2SO_4]_{0.3300}$	-6.45	2109	17.5	0.9913
$[C_2MIM]$ $[SCN]_{0.3200}[C_2SO_4]_{0.6800}$	-6.93	1978	16.4	0.9914

$[C_2MIM][C_2SO_4]$	-7.24	1857	15.4	0.9967

Table A9 Fitted parameters of the linear expression given by Equation 2.3

Ionic Liquid Sample	$\ln(\sigma_0)$	-Ea/R	-Ea/ $Jmol^{-1}$ ($x10^{-3}$)	r^2
$[C_2MIM]\ [SCN]_{0.8990}\ [C_2SO_4]_{0.1010}$	26.34	0.027	0.22	0.9975
$[C_2MIM]\ [SCN]_{0.6700}[C_2SO_4]_{0.3300}$	17.24	0.030	0.24	0.9984
$[C_2MIM]\ [SCN]_{0.3200}[C_2SO_4]_{0.6800}$	8.84	0.035	0.29	0.9992
$[C_2MIM][C_2SO_4]$	5.21	0.039	0.32	0.9994

Appendix B

Table B1 Experimental data in mass fraction (w) and molar fraction(x) of the binodal curve for the ternary system heptane (1) + ethanol (2) + [C_2MIM][SCN] (3) at 298.15K and atmospheric pressure and the respective densities and refractive indices

w_1	w_2	w_3	x_1	x_2	x_3	ρ (g.cm^{-3})	n_D
0.0000	0.0000	1.0000	0.0000	0.0000	1.0000	1.112980	1.549260
1.0000	0.0000	0.0000	1.0000	0.0000	0.0000	0.675410	1.382860
0.0000	1.0000	0.0000	0.0000	1.0000	0.0000	0.781590	1.357340
0.9871	0.0129	0.0000	0.9723	0.0277	0.0000	0.680483	1.384863
0.9790	0.0210	0.0000	0.9555	0.0445	0.0000	0.680850	1.384610
0.9514	0.0486	0.0000	0.9000	0.1000	0.0000	0.683450	1.383507
0.9159	0.0841	0.0000	0.8336	0.1664	0.0000	0.686893	1.382510
0.8912	0.1064	0.0024	0.7929	0.2059	0.0013	0.687270	1.382010
0.8328	0.1633	0.0039	0.6996	0.2984	0.0019	0.694803	1.379907
0.7791	0.2167	0.0042	0.6218	0.3762	0.0020	0.698260	1.378660
0.7339	0.2583	0.0078	0.5644	0.4321	0.0035	0.703923	1.378710
0.6477	0.3297	0.0226	0.4699	0.5204	0.0097	0.715170	1.385297
0.5395	0.4161	0.0444	0.3668	0.6154	0.0179	0.732673	1.383540
0.4952	0.4478	0.0570	0.3295	0.6481	0.0225	0.740670	1.383620
0.3743	0.5231	0.1025	0.2380	0.7234	0.0386	0.765957	1.385150
0.3108	0.5556	0.1336	0.1944	0.7561	0.0495	0.782117	1.387610
0.2740	0.5710	0.1550	0.1704	0.7725	0.0571	0.792497	1.390923
0.2231	0.5818	0.1951	0.1391	0.7889	0.0720	0.809867	1.395423
0.1871	0.5851	0.2278	0.1173	0.7981	0.0846	0.824150	1.400213
0.1524	0.5868	0.2608	0.0962	0.8062	0.0975	0.837960	1.405650
0.1221	0.5724	0.3055	0.0789	0.8043	0.1168	0.859827	1.414480
0.1030	0.5588	0.3383	0.0678	0.8003	0.1319	0.870520	1.418920
0.0855	0.5369	0.3776	0.0579	0.7907	0.1514	0.884940	1.428293
0.0629	0.5144	0.4227	0.0439	0.7813	0.1748	0.902587	1.434480
0.0556	0.4972	0.4473	0.0396	0.7714	0.1889	0.914753	1.440377
0.0435	0.4740	0.4825	0.0320	0.7580	0.2100	0.924867	1.444263
0.0353	0.4504	0.5144	0.0267	0.7425	0.2308	0.937687	1.451470
0.0321	0.4256	0.5423	0.0251	0.7238	0.2511	0.947303	1.455917
0.0262	0.3606	0.6132	0.0223	0.6683	0.3093	0.972680	1.470453
0.0210	0.3226	0.6563	0.0189	0.6314	0.3497	0.990327	1.479050
0.0181	0.2791	0.7028	0.0173	0.5831	0.3996	1.006490	1.488777
0.0137	0.2361	0.7502	0.0141	0.5287	0.4572	1.023010	1.497760
0.0120	0.1947	0.7933	0.0133	0.4678	0.5189	1.040160	1.506383
0.0111	0.1319	0.8570	0.0138	0.3563	0.6299	1.064673	1.521703
0.0099	0.0816	0.9085	0.0137	0.2447	0.7416	1.085140	1.532593

Table B2 Experimental data in mass fraction (w) and molar fraction(x) of the binodal curve for the ternary system heptane (1) + ethanol (2) +$[C_2MIM][SCN]_{0.9}[C_2SO_4]_{0.1}$ (3) at 298.15K and atmospheric pressure.

w_1	w_2	w_3	x_1	x_2	x_3	ρ (g.cm^{-3})	n_D
0.0000	0.0000	1.0000	0.0000	0.0000	1.0000	1.118360	1.549560
1.0000	0.0000	0.0000	1.0000	0.0000	0.0000	0.679890	1.385370
0.0000	1.0000	0.0000	0.0000	1.0000	0.0000	0.781590	1.357340
0.9901	0.0099	0.0000	0.9788	0.0212	0.0000	0.680260	1.385063
0.9878	0.0122	0.0000	0.9739	0.0261	0.0000	0.680430	1.384987
0.9705	0.0295	0.0000	0.9380	0.0620	0.0000	0.681667	1.384410
0.9515	0.0485	0.0000	0.9002	0.0998	0.0000	0.683077	1.383723
0.9121	0.0879	0.0000	0.8266	0.1734	0.0000	0.686300	1.382563
0.8481	0.1519	0.0000	0.7196	0.2804	0.0000	0.691770	1.380670
0.7999	0.2001	0.0000	0.6475	0.3525	0.0000	0.696097	1.379387
0.7449	0.2486	0.0064	0.5779	0.4196	0.0025	0.703217	1.379257
0.6925	0.2964	0.0111	0.5158	0.4801	0.0041	0.708807	1.378050
0.6533	0.3266	0.0200	0.4756	0.5172	0.0072	0.714810	1.378313
0.6008	0.3680	0.0311	0.4241	0.5651	0.0109	0.721940	1.384273
0.5211	0.4237	0.0551	0.3545	0.6270	0.0185	0.736580	1.383270
0.4500	0.4703	0.0797	0.2975	0.6764	0.0260	0.750993	1.383413
0.4021	0.5011	0.0968	0.2611	0.7078	0.0311	0.760870	1.383837
0.3456	0.5316	0.1228	0.2212	0.7400	0.0388	0.774637	1.386120
0.3233	0.5442	0.1325	0.2056	0.7528	0.0416	0.779990	1.387263
0.2889	0.5654	0.1458	0.1816	0.7731	0.0453	0.787687	1.389103
0.2535	0.5763	0.1702	0.1593	0.7878	0.0529	0.798647	1.392240
0.2275	0.5860	0.1865	0.1427	0.7995	0.0578	0.806587	1.394403
0.2064	0.5896	0.2040	0.1298	0.8068	0.0634	0.814380	1.396640
0.1862	0.5876	0.2262	0.1182	0.8109	0.0709	0.824813	1.399853
0.1673	0.5837	0.2490	0.1072	0.8139	0.0789	0.833120	1.403783
0.1422	0.5826	0.2752	0.0920	0.8200	0.0880	0.844247	1.407513
0.1278	0.5769	0.2953	0.0836	0.8209	0.0954	0.853553	1.412807
0.1105	0.5611	0.3284	0.0740	0.8173	0.1087	0.867380	1.414583
0.0847	0.5332	0.3820	0.0591	0.8092	0.1317	0.890993	1.424693
0.0674	0.5110	0.4216	0.0486	0.8012	0.1502	0.903887	1.431410
0.0513	0.4868	0.4619	0.0383	0.7911	0.1706	0.921657	1.437977
0.0444	0.4596	0.4960	0.0344	0.7755	0.1901	0.933523	1.442967
0.0395	0.4358	0.5247	0.0317	0.7603	0.2080	0.944297	1.448433
0.0303	0.3950	0.5747	0.0259	0.7321	0.2420	0.965730	1.459367
0.0222	0.3401	0.6376	0.0206	0.6869	0.2925	0.989107	1.468600